Application of Calorimetric Low Temperature Detectors for the Investigation of Z-Yield Distributions of Fission Fragments and for other Research Topics

Peter Egelhof

GSI Helmholtzzentrum für Schwerionenforschung, Darmstadt, Germany
and
University Mainz, Germany

Seminar

PNPI Gatchina, Russia
November 28, 2017

I. Introduction

II. Detection Principle and Basic Properties of Calorimetric Low Temperature Detectors (CLTD`s)

III. CLTD`s for High Resolution Detection of Heavy Ions - Design and Performance

IV. Investigation of Z-Yield Distributions of Fission Fragments

V. Other Applications in Heavy Ion Physics

VI. Conclusions

I. Introduction

The success of experimental physics and the quality of the results generally depends on the quality of the available detection systems !

⇒ idea: detection of radiation independent of ionisation processes

⇨ calorimetric detector

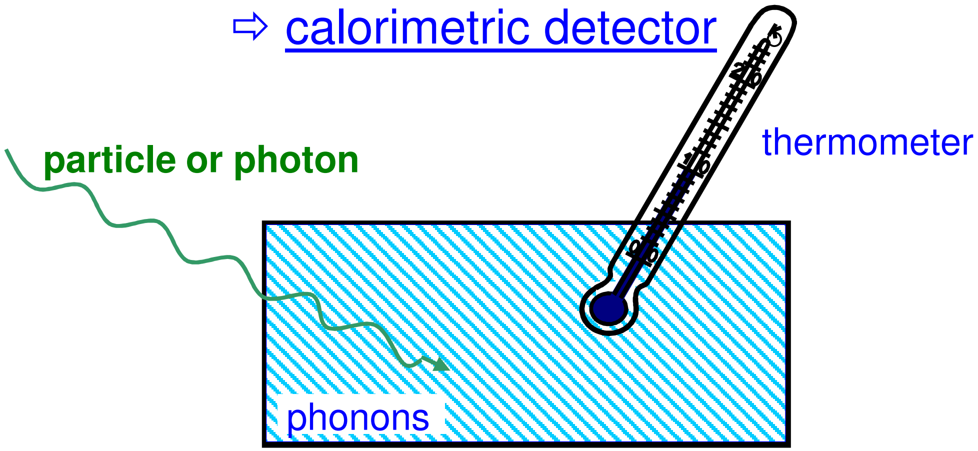

interaction of radiation with matter:

primary: ionization, ballistic phonons
(conventional ionisation detectors)

secondary: thermalization:
conversion of energy to heat

⇒ detection of thermal phonons

⇒ calorimetric detectors

potential advantage:

- energy resolution
- energy linearity
- detection threshold
- radiation hardness

⇒ various applications in many fields of physics

Applications of Low Temperature Detectors - an Overview

Astrophysics:

- dark matter
  ⇒ low detection threshold
- solar neutrinos
  ⇒ low detection threshold
- cosmic x-rays
  ⇒ high energy resolution

Particle physics:

- $\beta\beta0\nu$-decay
  ⇒ absorber = source (^{130}Te)
- neutrino mass from β- endpoint determ.
  ⇒ absorber = source (^{187}Re)

Atomic and Nuclear physics:

- X-ray detection
  ⇒ high energy resolution
- Ion detection
  ⇒ high energy resolution
  ⇒ good energy linearity

Applied physics:

- x-ray material analysis
  ⇒ high energy resolution
- life sciences (MALDI)
  ⇒ high energy resolution

for more detailed information see:

- Cryogenic Particle Detection,
  Topics in Applied Physics 99 (2005)
- Proceedings 16th Int. Workshop on
  Low Temperature Detectors,
  JLTP 184 (2016), ~300 participants!

Low Temperature Detectors (LTD`s) for Atomic, Nuclear and Particle Physics

- needed for atomic, nuclear and particle physics:
  - ⇒ energy sensitive detectors for x-rays, γ-rays
  - ⇒ energy sensitive detectors for particles

- the concept of LTD`s provides substantial advantage over conventional detection schemes with respect to basic detector properties:
  - ⇒ energy resolution
  - ⇒ energy linearity
  - ⇒ detection threshold
  - ⇒ dynamic range
  - ⇒ radiation hardness

- LTD`s have a large potential for various applications in basic and applied Heavy Ion Research:
  - ⇒ Nuclear Structure and Astrophysics
  - ⇒ Atomic Physics
  - ⇒ Symmetries and Basic Interactions
  - ⇒ Interaction of Radiation with Matter

II. Detection Principle and Basic Properties of Calorimetric Low Temperature Detectors (CLTD`s)

detection principle:

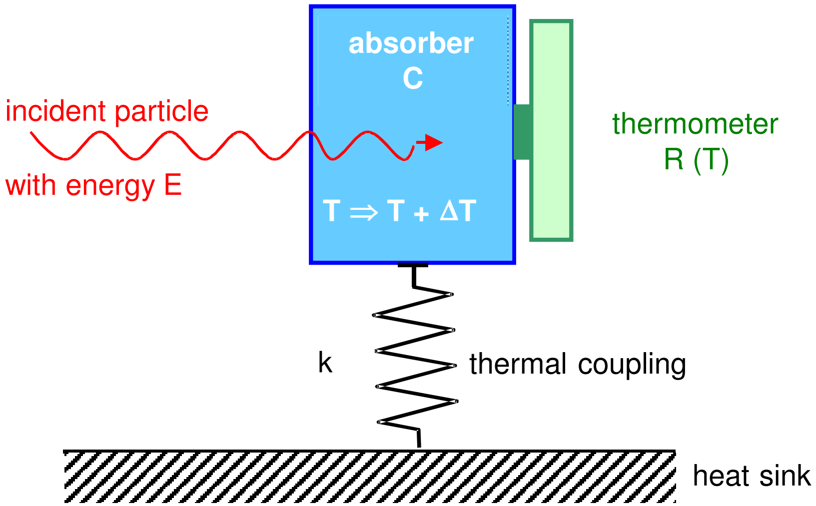

thermal signal:

after particle absorption and decay of excited electronic states ($\approx 10^{-8}$ sec):

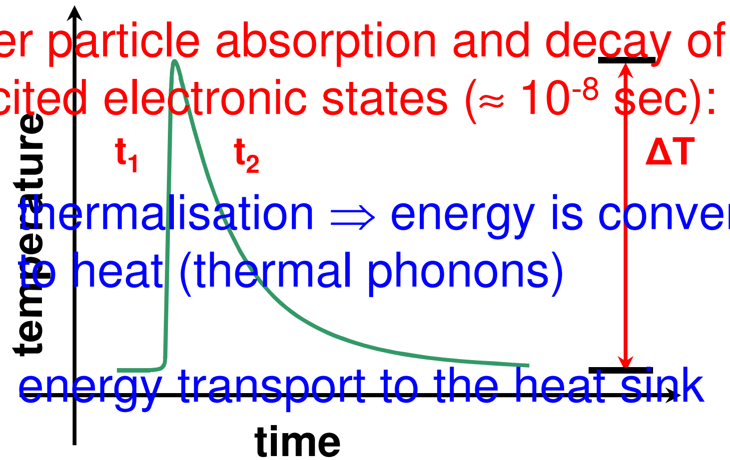

- thermalisation $\Rightarrow$ energy is converted to heat (thermal phonons)
- energy transport to the heat sink

amplitude:	$\Delta T = E/C$	($C = c \bullet m$ = heat capacity)
rise time:	$\tau_1 \geq \tau_{therm}$	($\approx$ 1 – 10 μsec)
fall time:	$\tau_2 = C/k$	($\approx$ 100 μsec – 10 msec)

Optimization of the Sensitivity

a) <u>absorber:</u> maximum sensitivity $\Delta T = E/mc$ for

– small absorber mass m

– small specific heat c

due to: $c = \underbrace{\cancel{\alpha\, T}}_{\text{electrons}} + \underbrace{\beta\, (T/\theta_D)^3}_{\text{lattice}}$ (θ_D = Debye-temperature)

$\Rightarrow$ low operating temperature $\Rightarrow$ „<u>low-temperature detector</u>“

(αT dominating for $T \leq 10K \Rightarrow$ insulators ($\alpha = 0$) or superconductors)

b) <u>thermometer:</u> for thermistor (bolometer): $\Delta T \rightarrow \Delta R \rightarrow \Delta U$

$\Rightarrow$ maximum sensitivity for large dR/dT

– semiconductor thermistor

due to appropriate doping $\Rightarrow$ exponential behavior of R(T)

– superconducting phase transition thermometer

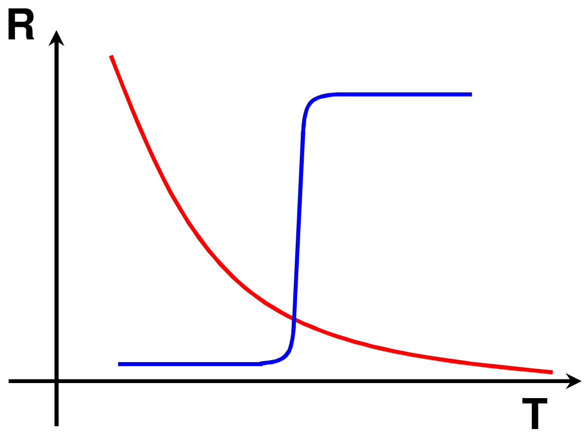

Potential Advantage over Conventional Detectors

- small energy gap ω

  ⇒ better statistics of the detected phonons

  semiconductor detector: $\omega \approx 1$ eV

  calorimetric detector: $\omega \leq 10^{-3}$ eV

$$\frac{\Delta E_{calorimeter}}{\Delta E_{semicond.\mathrm{det}.}} = \sqrt{\frac{N_{electr.}}{N_{phon.}}} = \sqrt{\frac{\omega_{phon}}{\omega_{electr.}}} \leq \frac{1}{30}$$

- more complete energy detection ⇒ better linearity and resolution

  energy deposited in phonons and ionisation contributes to the signal
  (for ionisation detectors: losses up to 60-80% due to: - recombination
  - direct phonon production)

- small noise power at low temperatures

- method independent on absorber material

  ⇒ optimize radiation hardness, absorption efficiency, etc.

Theoretical Limit for the Energy Resolution

for ideal calorimetric detector:

- thermodynamic fluctuations (quantum statistics)
- Johnson noise
- amplifier noise

$$\Rightarrow \langle \Delta E \rangle = \underbrace{\xi}_{\text{noise}} \bullet \underbrace{\sqrt{k_B T^5 c\, m}}_{\text{thermodynamic fluctuations}} \qquad 1 < \xi < 3$$

example: 1 MeV particle in a 1 mm^3 sapphire absorber

T	C	ΔT	ΔE_{theor}
300 K	$3 \bullet 10^{-3}$ J/K	$5 \bullet 10^{-11}$ K	1.8 GeV
10 K	$4 \bullet 10^{-7}$ J/K	$4 \bullet 10^{-7}$ K	700 keV
1 K	$4 \bullet 10^{-10}$ J/K	0.4 mK	2.2 keV
100 mK	$4 \bullet 10^{-13}$ J/K	400 mK	7 eV

⇒ for low temperature: microscopic particle affects the properties of a macroscopic absorber

Theoretical Limit for the Energy Resolution

for ideal calorimetric detector:

- thermodynamic fluctuations (quantum statistics)
- Johnson noise
- amplifier noise

$$\Rightarrow \; <\Delta E> = \underset{\text{noise}}{\xi} \bullet \underbrace{\sqrt{k_B T^5 c\; m}}_{\text{thermodynamic fluctuations}} \qquad 1 < \xi < 3$$

example: 50 keV X-ray, 1 mm^2 tin absorber with a thickness of 50 μm

T	C	ΔT	$\Delta E_{theor.}$
300 K	$8 \cdot 10^{-5}$ J/K	$1 \cdot 10^{-10}$ K	295 MeV
1 K	$1{,}2 \cdot 10^{-9}$ J/K	$6{,}7 \cdot 10^{-6}$ K	3,8 keV
0,1 K	$1{,}2 \cdot 10^{-12}$ J/K	$6{,}7 \cdot 10^{-3}$ K	12 eV
0,05 K	$1{,}5 \cdot 10^{-13}$ J/K	$5{,}3 \cdot 10^{-2}$ K	2 eV

(theoretical limit for a conventional semiconductor detector: $\Delta E_{theor} = 350$ eV)

$\Rightarrow$ for low temperature: microscopic photon affects the properties of a macroscopic absorber

III. CLTD`s for High Resolution Detection of Heavy Ions - Design and Performance

Detector Design and Perfomance:

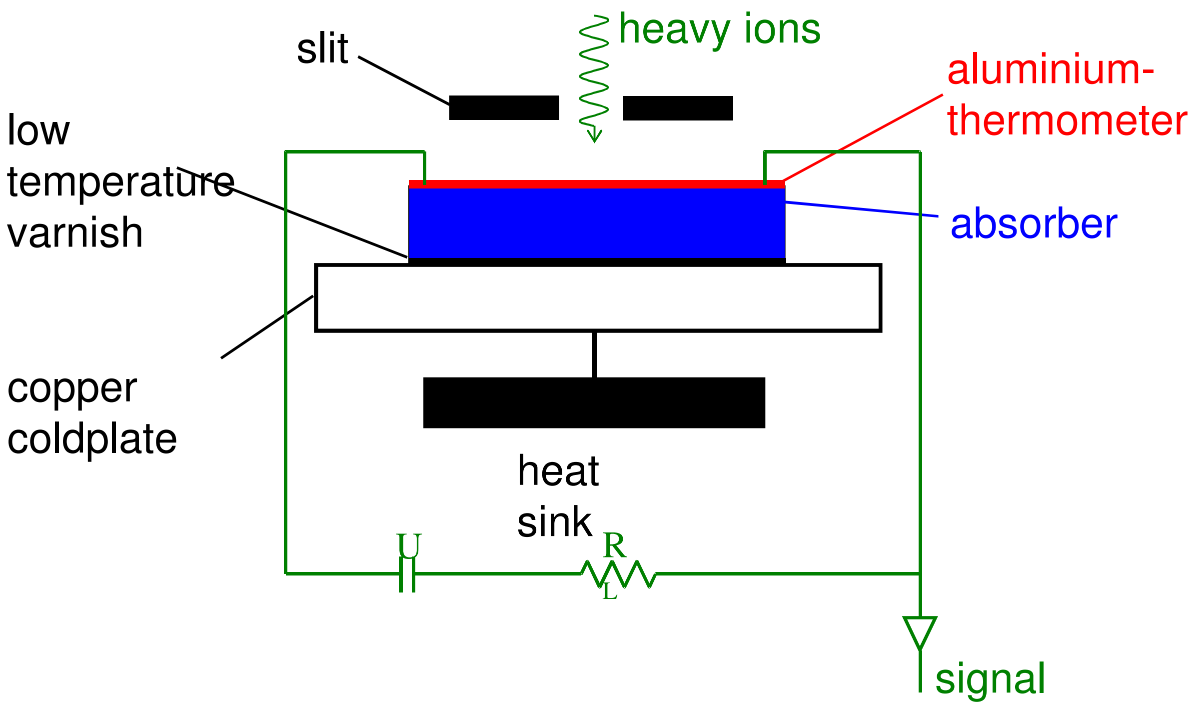

for an overview see:

P.E. and S. Kraft-Bermuth,

Top. Appl. Phys. 99 (2005) 469

absorber: sapphire-crystal: V= 3 x 3 mm² x 430 µm

thermometer: aluminium-film (d = 10 nm), $T_C \approx 1.5°K$ (in the range of a ^{4}He-cryostat)
(for impedance matching to the amplifier: ⇒ meander structure)

readout: conventional pulse electronics +Flash-ADC`s +Digital Filtering

III. CLTD`s for High Resolution Detection of Heavy Ions - Design and Performance

Detector Design and Perfomance:

for an overview see:
P.E. and S. Kraft-Bermuth, Top. Appl. Phys. 99 (2005) 469

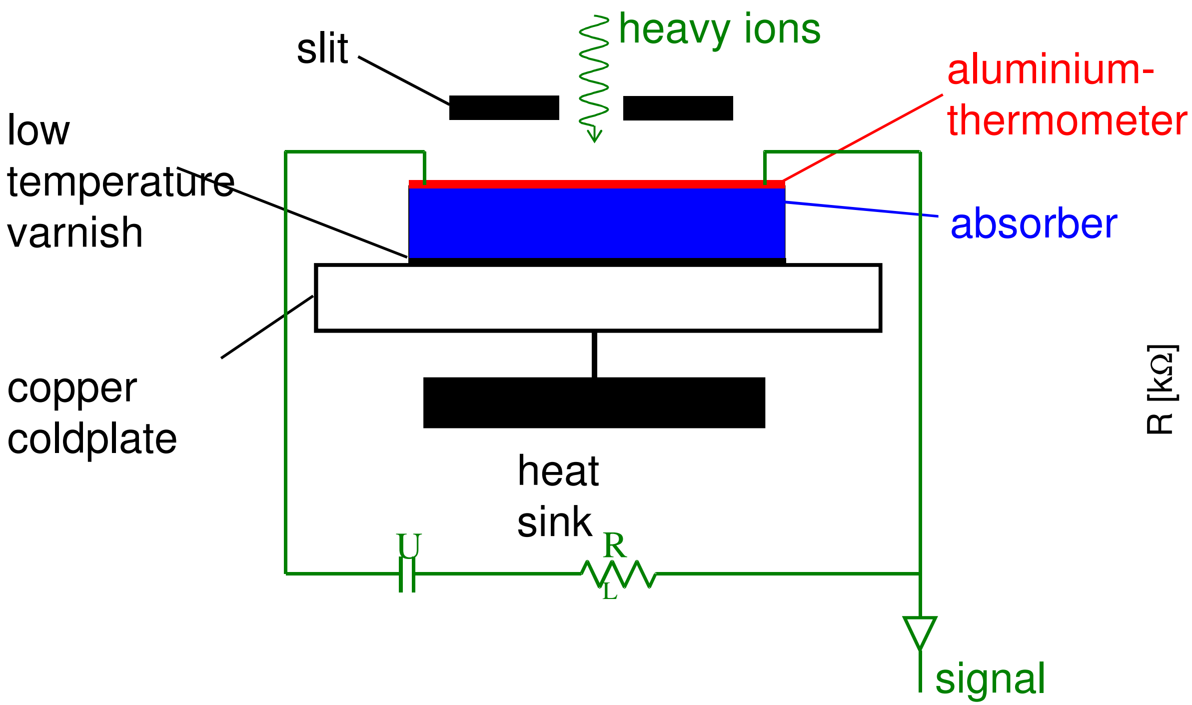

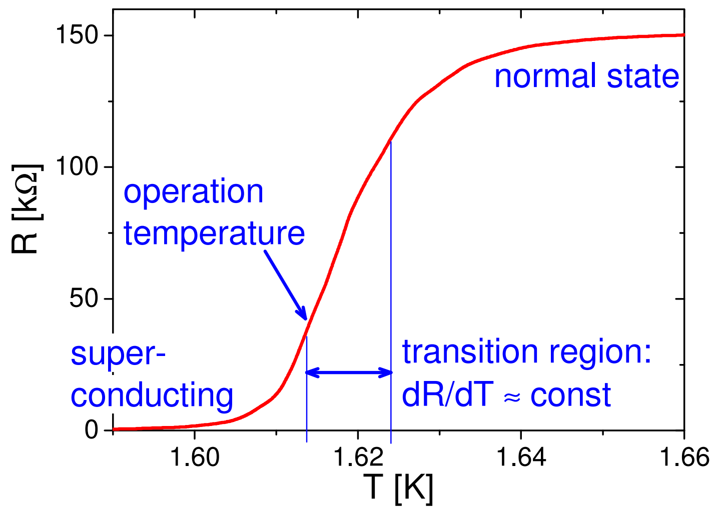

absorber: sapphire-crystal: V= 3 x 3 mm² x 430 µm

thermometer: aluminium-film (d = 10 nm), $T_C \approx 1.5°K$ (in the range of a ^4He-cryostat)
(for impedance matching to the amplifier: ⇒ meander structure)

readout: conventional pulse electronics +Flash-ADC`s +Digital Filtering

CLTD`s for High Resolution Detection of Heavy Ions - Design and Performance

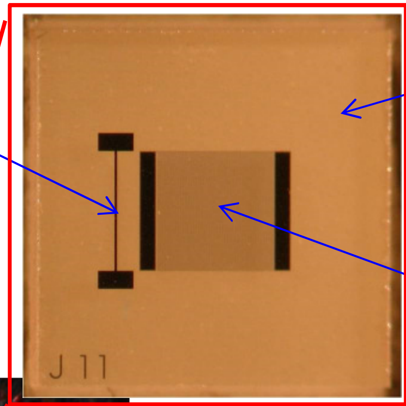

detector pixel:

- absorber:
  $3 \times 3 \times 0.43$ mm^3 sapphire (Al_2O_3)
- thermometer:
  Transition Edge Sensor (TES)
  10 nm thick meander shaped Al-layer
  $\Rightarrow$ photolithography (high purity!!)
- heating resistor:
  Au/Cr strip
- operation temperature:
  $T_c = 1.5 - 1.6$ K

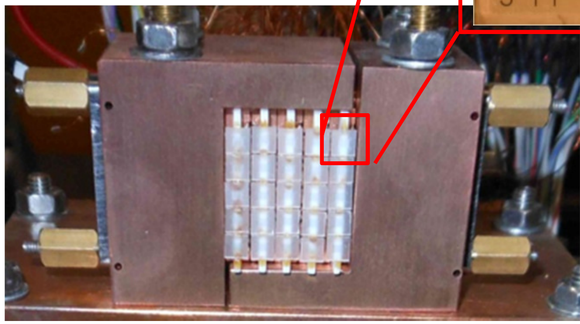

CLTD-array

cryostat

detector array:

- 25 pixels with individual temperature stabilization in operation
- active area: 1.5 cm x 1.5 cm
- windowless coupling of cryostat to beam line

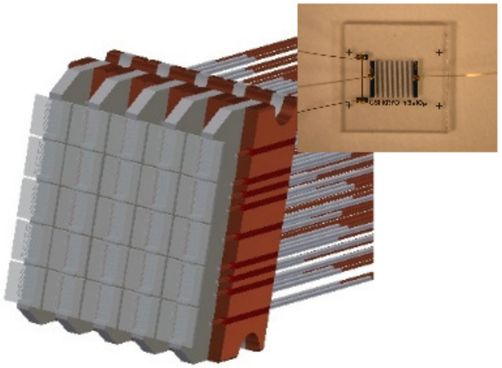

New Large Solid Angle Detector Array

number of pixels: 25

active area: 15 X 15 mm^2

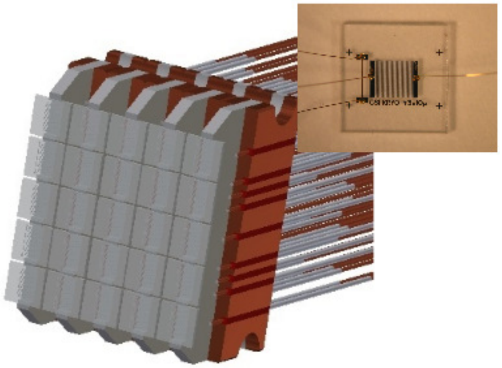

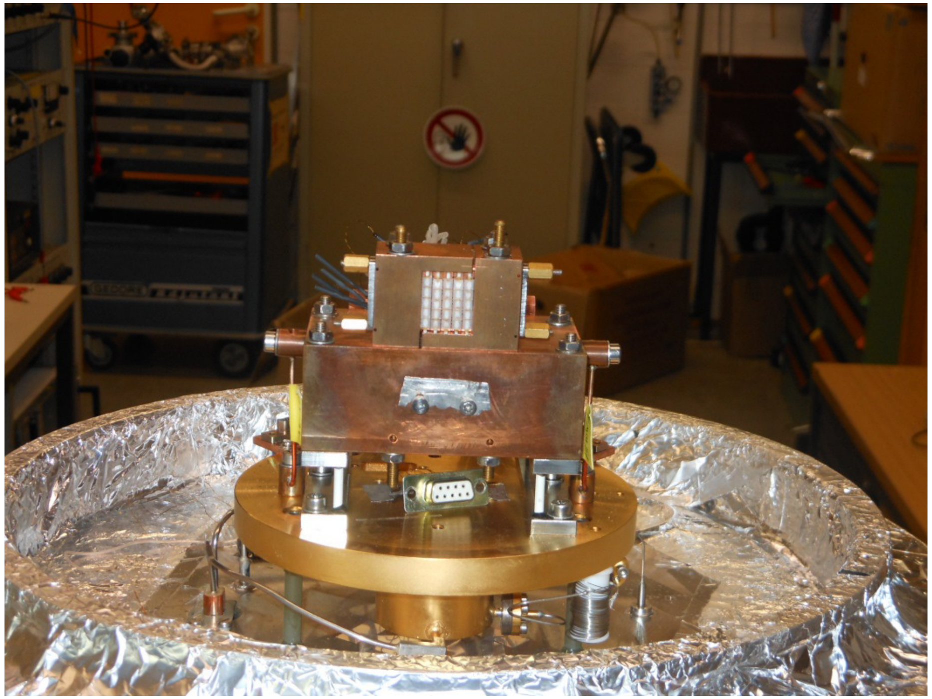

CLTD`s for High Resolution Detection of Heavy Ions - Design and Performance

detector performance: response to ^{32}S ions @ 100 MeV

rate capability:

$\geq$ 200 sec^{-1}

resolution:

$\Delta E/E = 1.6 \times 10^{-3}$

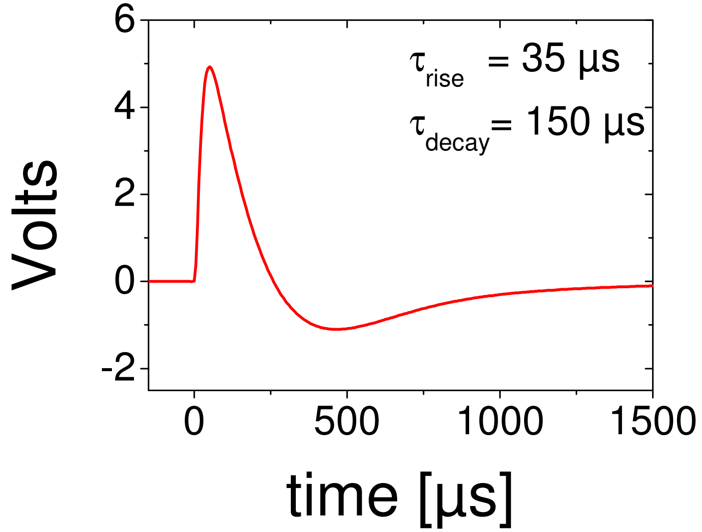

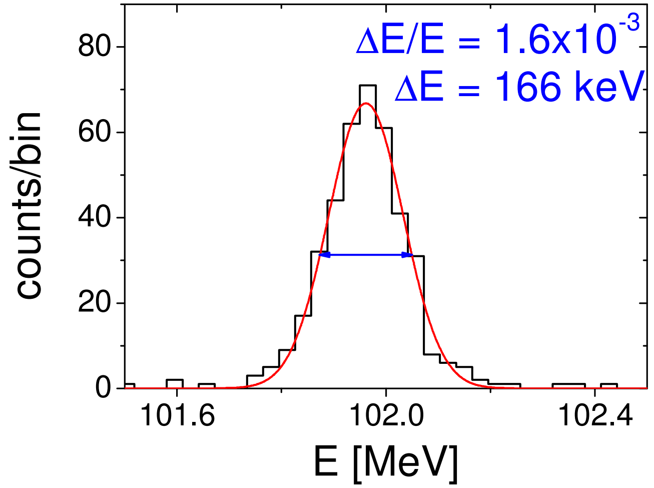

systematical investigation of energy resolution:

with UNILAC-beam: for ^{209}Bi, E = 11.6 MeV/u $\Rightarrow$ $\Delta E/E = 1.8 \times 10^{-3}$

with ESR-beam: for ^{238}U, E = 360 MeV/u $\Rightarrow$ $\Delta E/E = 1.1 \times 10^{-3}$

with Tandem-beam: for ^{152}Sm, E = 3.6 MeV/u $\Rightarrow$ $\Delta E/E = 1.6 \times 10^{-3}$

$\Rightarrow$ for heavy ions: $\geq$ 20 x improvement over conventional Si detectors

Comparison of Detector Performance: CLTD – Conventional Si Detector

<u>energy resolution:</u>

example:

^{238}U @ 20.7 MeV)

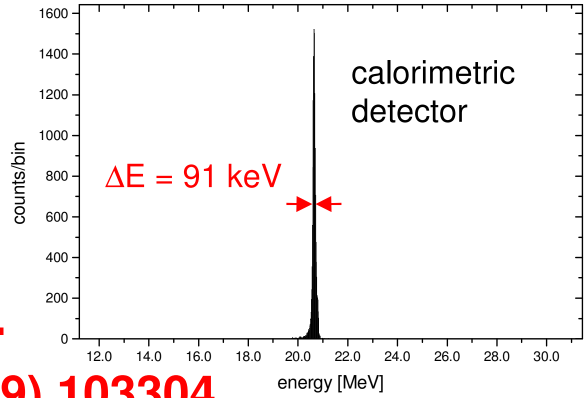

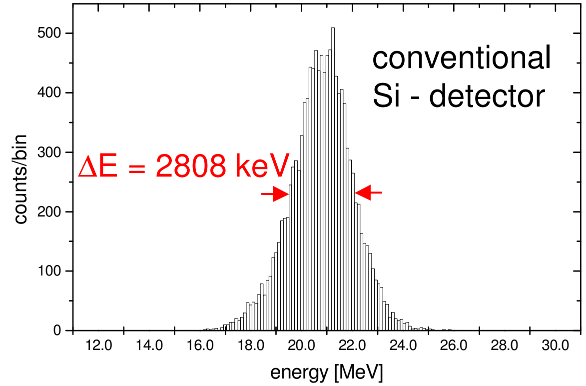

S. Kraft-Bermuth et al.

Rev. Sci. Instr. 80 (2009) 103304

<u>energy linearity:</u>

example:

^{13}C, ^{197}Au, ^{238}U

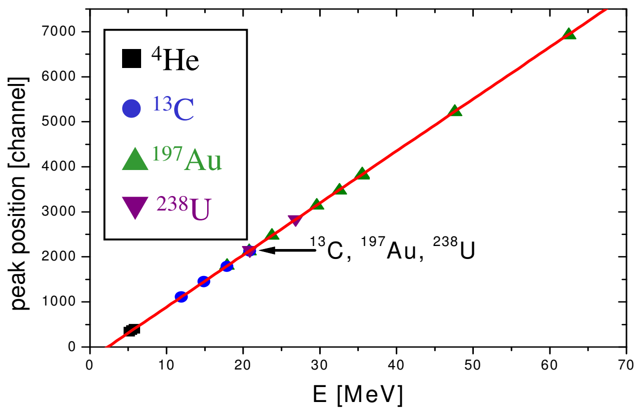

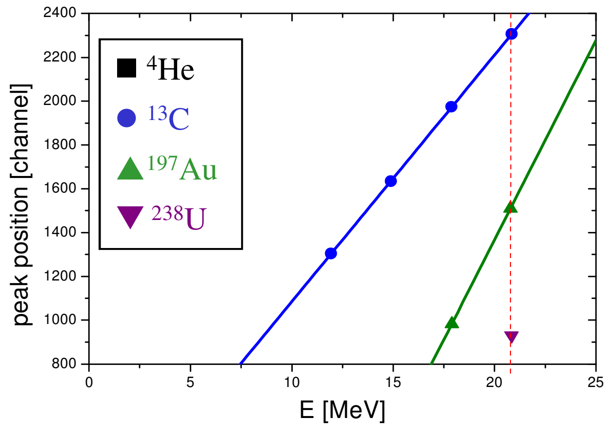

<u>for conventional ionization detector:</u>

high ionization density leads to charge recombination (E- and Z- dependent)

⇒ pronounced pulse height defects ⇒ nonlinear energy response

⇒ fluctuation of energy loss processes ⇒ limited energy resolution

Applications of CLTD`s in Heavy Ion Physics

- High Resolution Nuclear Spectroscopy
- Investigation of Stopping Powers of Heavy Ions in Matter
- In-Flight Mass Identification of Heavy Ions by E-TOF
- Accelerator Mass Spectrometry
- Lamb Shift Measurements in Hydrogen-Like Heavy Ions
- Investigation of Z-Yield Distributions of Fission Fragments

IV. Investigation of Z (Nuclear Charge)-Yield Distributions of Fission Fragments

- fission of ^{235}U, ^{239}Pu, ^{241}Pu induced by thermal neutrons:
  - ⇒ capture of a thermal neutron
  - ⇒ binary scission
  - ⇒ about 85% (~170 MeV) of the energy released is transferred to the kinetic energy of the fragments

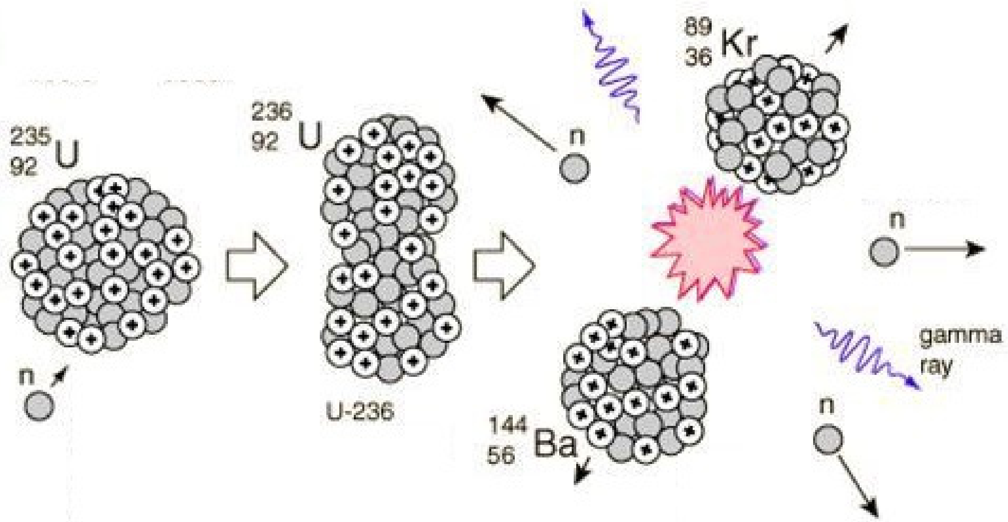

- motivation for studying properties of fission fragments:
  - ⇒ better understanding of the nuclear fission process (for example:odd-even staggering determines fission mode)
  - ⇒ test of theoretical predictions
  - ⇒ information about nuclear structure (shell effects, pair breaking, ...)
  - ⇒ data relevant for reactor physics (for example: reactor antineutrino anomaly)

Investigation of Z-Yield Distributions of Fission Fragments
a) Idea of the Experiment and Experimental Setup

- produce fission fragments by n $\rightarrow$ ^{235}U, $^{239,241}Pu$
  at the high flux research reactor of the ILL Grenoble

- select mass and energy in the LOHENGRIN mass separator

- identify Z by using the Z-dependent energy loss in an energy degrader
  (absorber method, see also U. Quade et al., NIM A164 (1979) 436
  U. Quade et al., Nucl. Phys. A487 (1988),1

- measure E_{rest} in a high resolving CLTD
  (instead of conventional ionization chamber limited by: energy resolution and pulse height defect)

Methods for Determination of Z-Yield Distributions of Fission Fragments

- Radio chemistry $\Rightarrow$ restricted to particular nuclides
- γ-spectroscopy $\Rightarrow$ disadvantage: indirect method (depends on knowledge of level schemes, branching ratios, lifetimes)

- Passive Absorber Method

U. Quade et al., Nucl. Phys. A487 (1988) 1

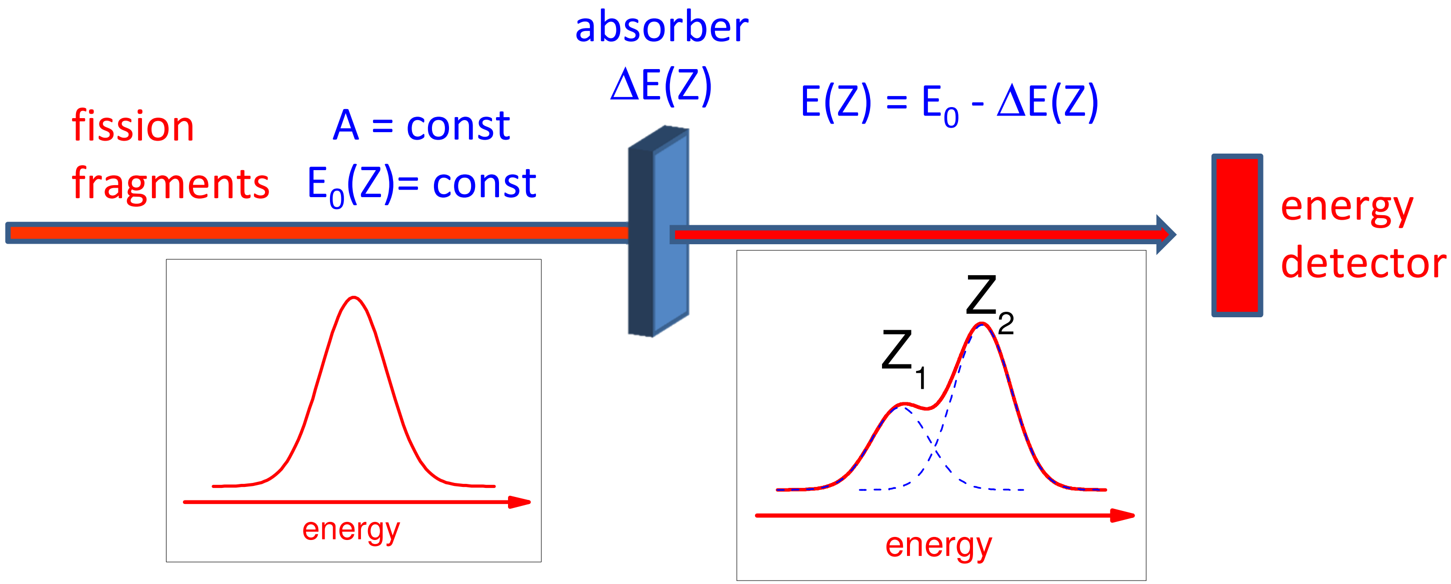

Idea of the Experiment: Investigation of Z (nuclear charge) Distributions of Fission Fragments

The LOHENGRIN Mass Separator at ILL Grenoble, France

- production of fission products by n → U, Pu
- separation according to A/Q (magnetic field) and E/Q (electric field)
- but no Z –selectivity!!

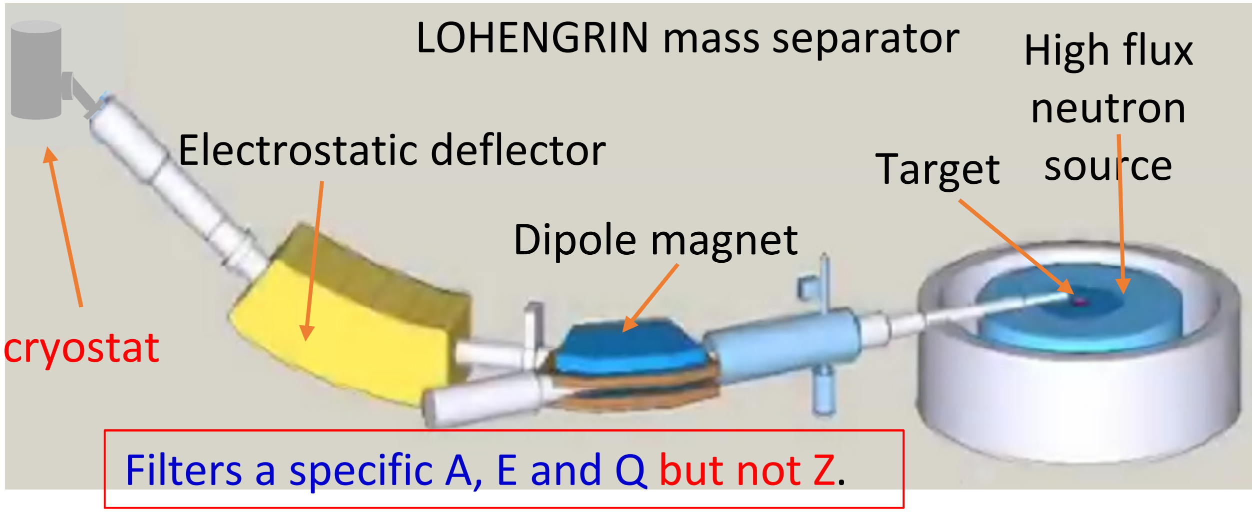

Z - Identification via the Absorber Method

Quality of Z – Separation depends on:

- proper choice of ΔE (absorber foil)
- homogenity of absorber foil
- energy resolution of CLTD`s

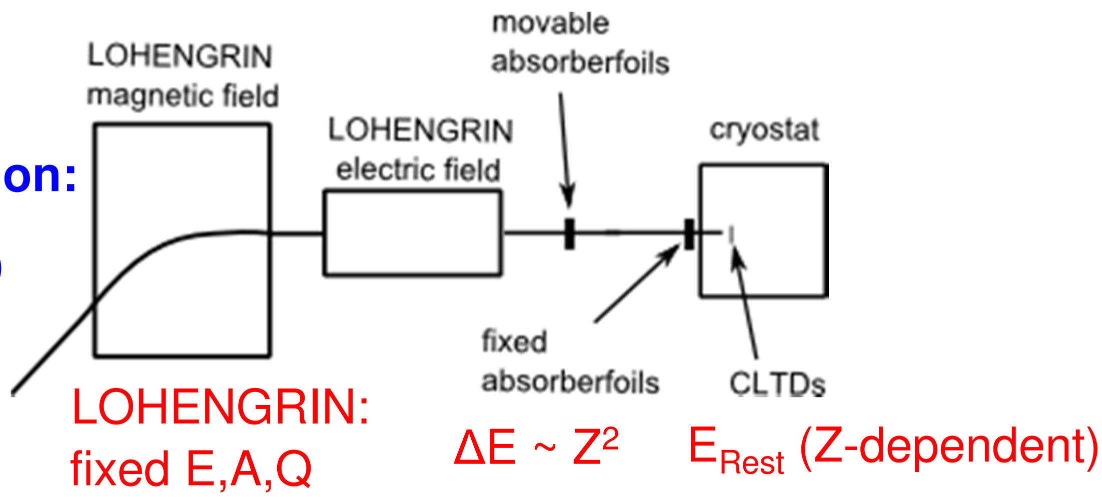

Feasibility Studies at the Munich Tandem Accelerator

- from the Tandem Accelerator:

  ⇒ stable beams of ^{109}Ag (E = 80 MeV)
  and ^{127}I (E = 68.7 MeV)
  (at same velocity)

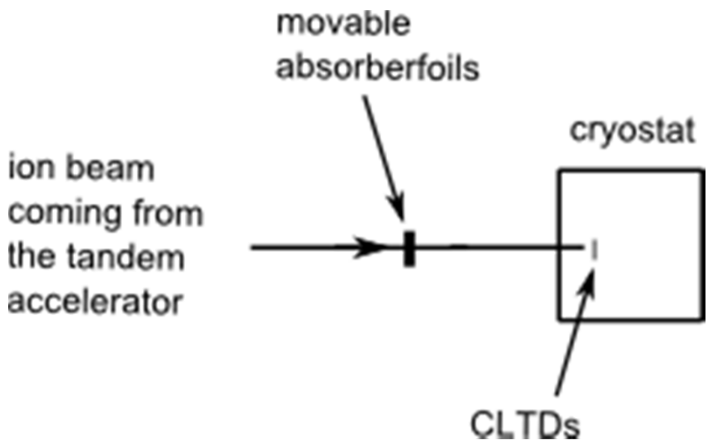

- aim of the experiment:

  ⇒ first test of the new 25 pixel array

  ⇒ check of quality of Z – separation dependent on:

  - type of absorber foil
  - thickness of absorber foil
  - homogenity of absorber foil
  - amount of energy straggling

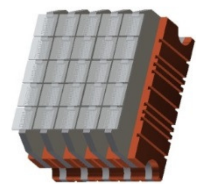

- **25 pixel CLTD array**
- **individual temperature stabilization**
- **active area ~ (15x15)mm²**

Energy Loss of ^{109}Ag in Si_3N_4 for different Thickness of the Absorber Foil

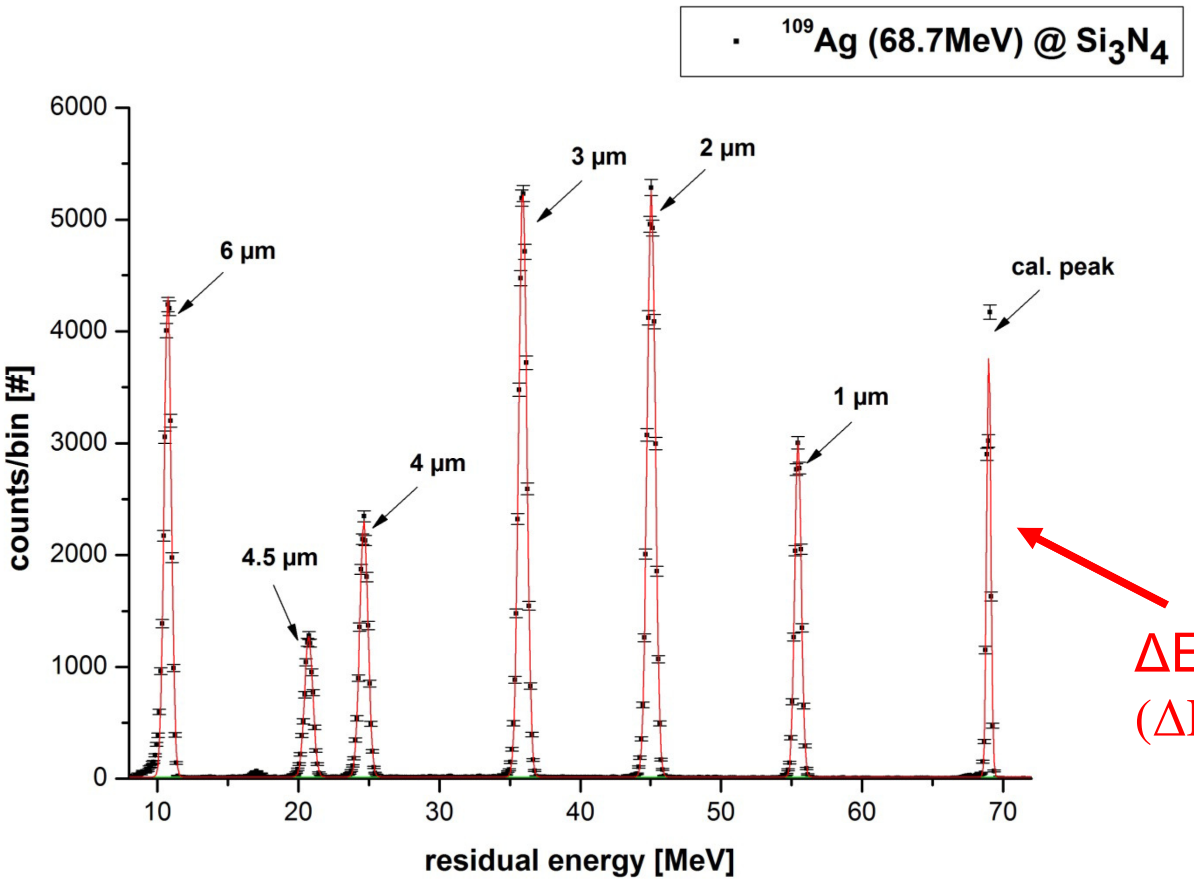

ΔE = 330 keV

(ΔE/E = 0.5 %)

FWHM for different Types of Absorber Foils

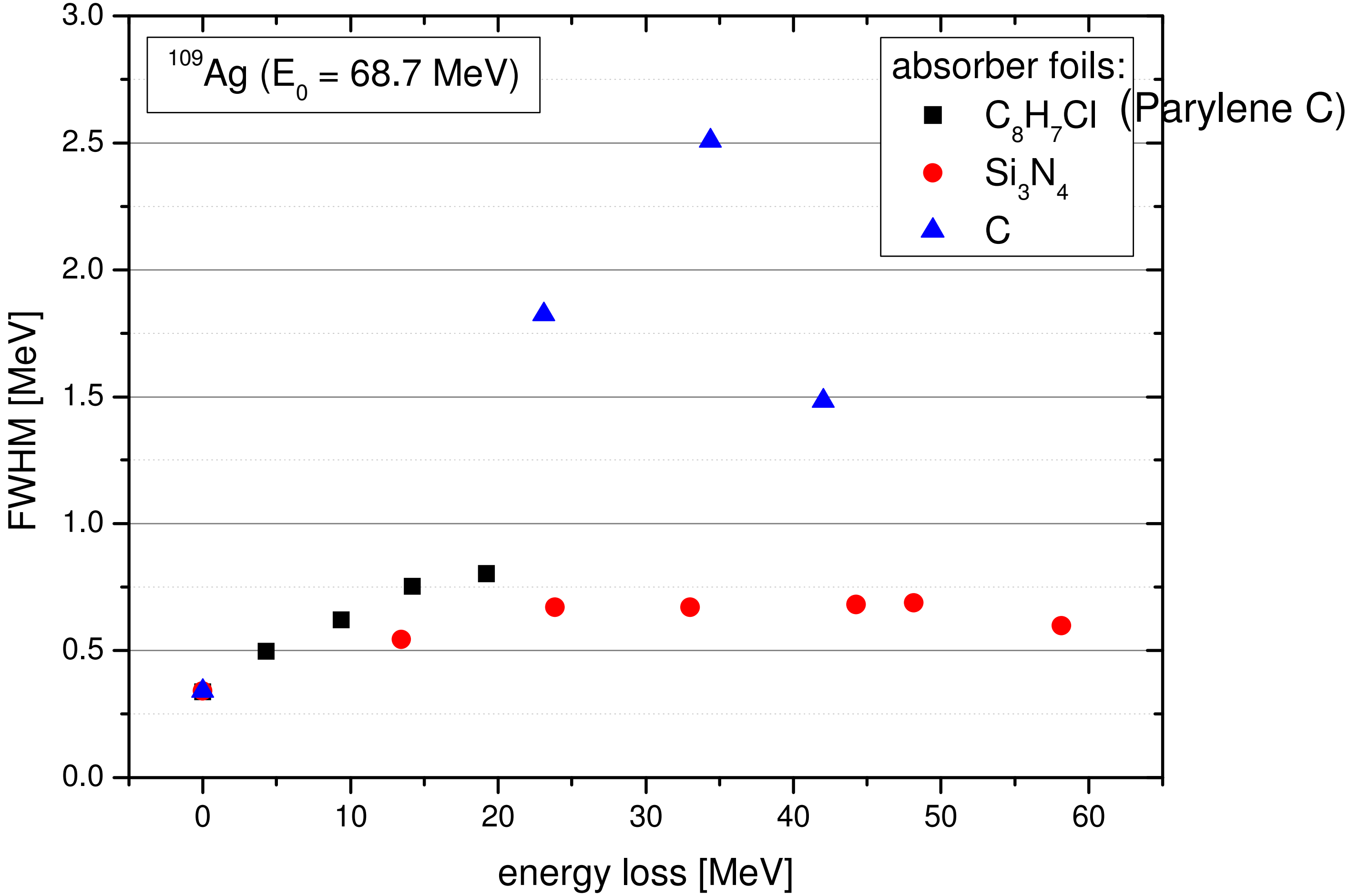

best performance found for Si_3N_4
as compared to previously used Parylene C

Experimental Setup at the ILL Reactor

- absorber foil: Si_3N_4
  good homogenity, small E- straggling
- manipulator for variable foil thickness (1-8 μm) for otimizing Z-resolution for different Z and E
- absorber foil integrated in cryostat for optimized efficiency

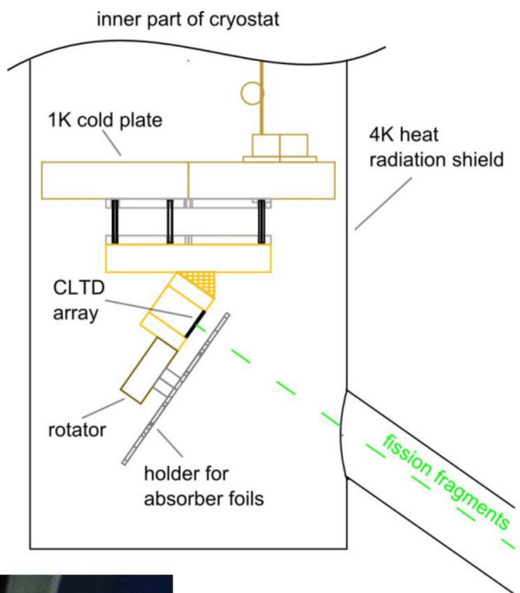

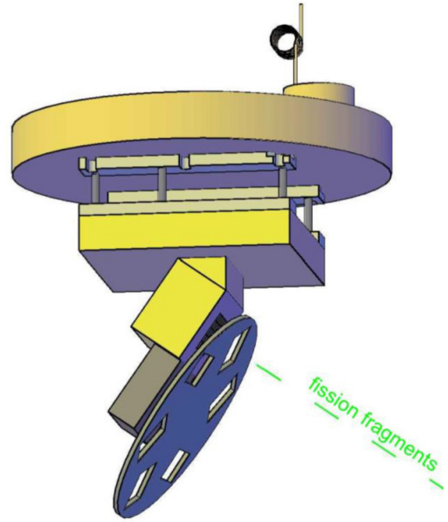

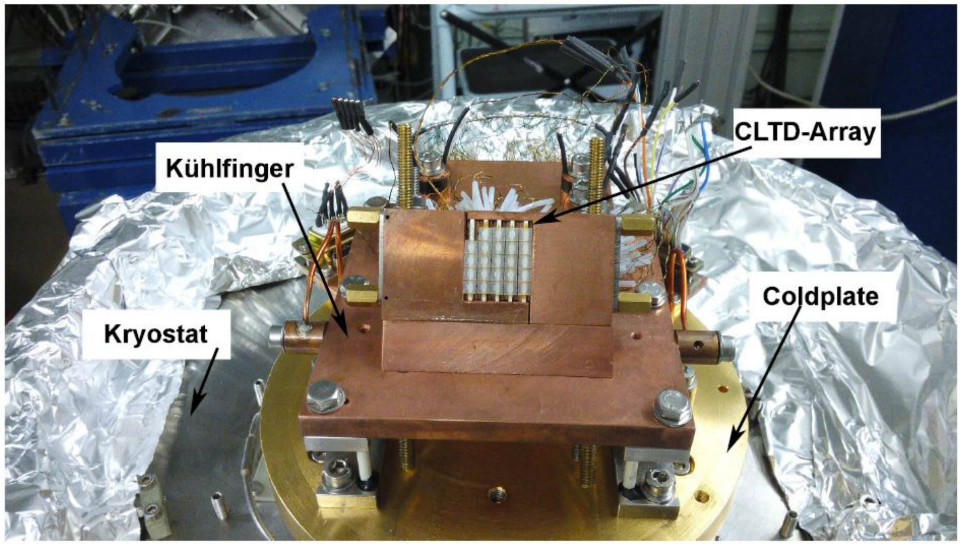

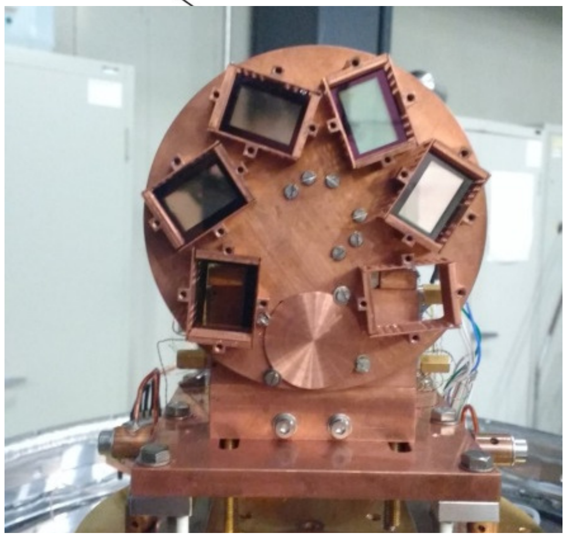

Investigation of Z-Yield Distributions of Fission Fragments
b) Results

- end of 2016: 5 weeks of beamtime at ILL
- rich harvest: Z-Yield Distributions for 3 Targets and 51 Masses

^{235}U(n_{th},f) (A=89,92,96,104-110,132.140)
^{241}Pu(n_{th},f) (A=89-91,92,96 97-112)
^{239}Pu(n_{th},f) (A=92,96,109-113, 128-137,139)

- substantial improvement of performance as compared to earlier investigations with conventional setups ⇒ first measurements in symmetry and heavy mass region

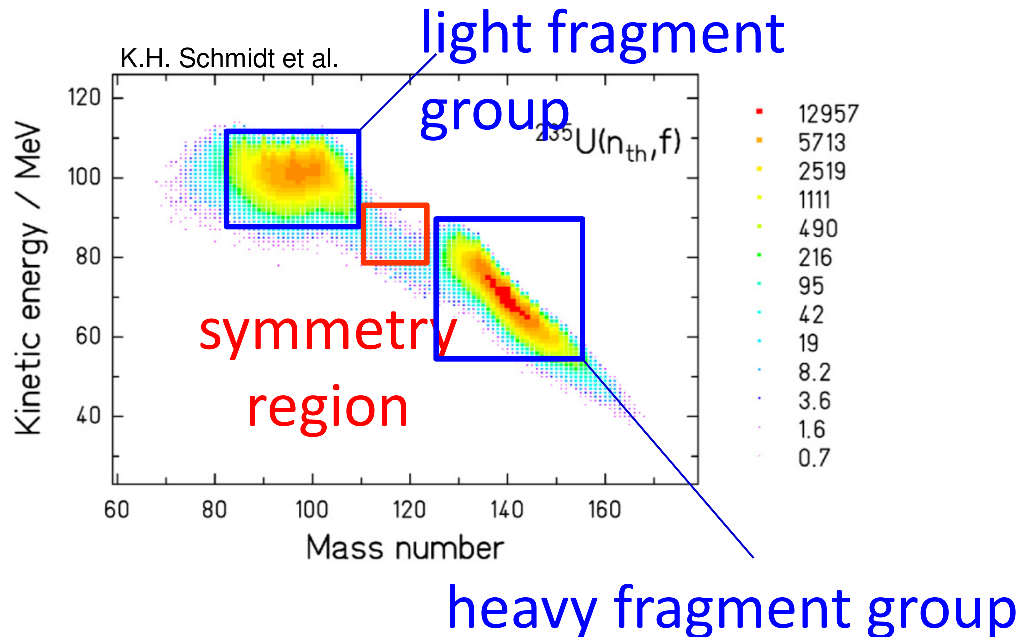

Quality of Z-Separation (figure of merit) dependent on Nuclear Mass A and Charge Z

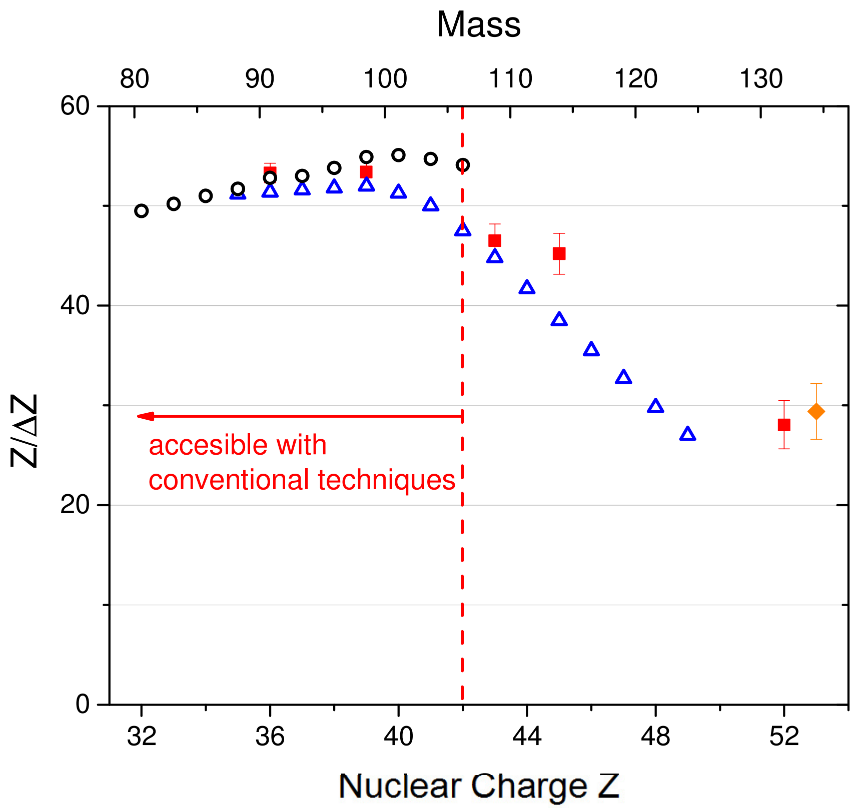

quality of separation ~ Z/ΔZ with

$$\Delta Z := \frac{\delta E(Z) - \delta E(Z-1)}{FWHM}$$

- ■ CLTD + Si_3N_4 (present data)
- ♦ CLTD + Si_3N_4 (test at Garching)
- ο IC + Parylene-C (Quade et al.)
- Δ IC + Parylene-C (prediction by Bocquet et al.)

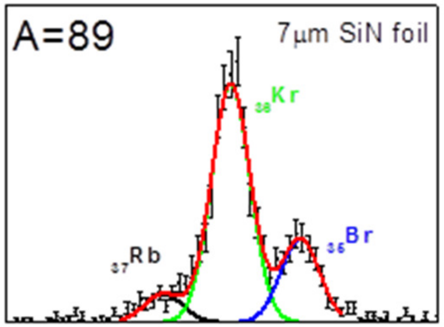

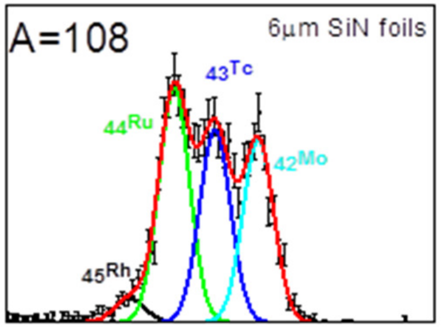

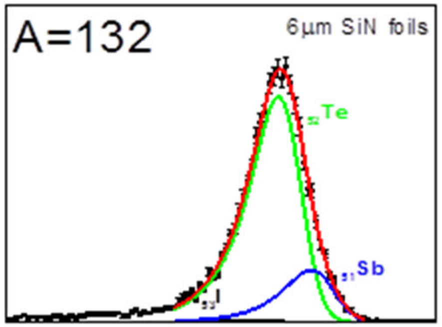

Quality of Z-Separation (figure of merit) dependent on Nuclear Mass A and Charge Z

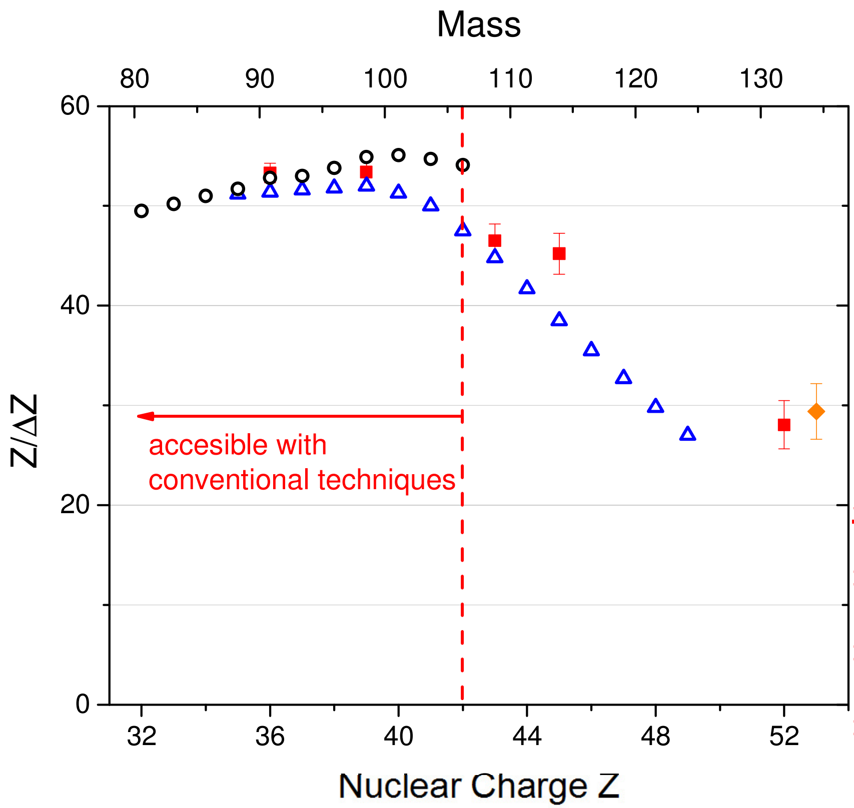

quality of separation ~ Z/ΔZ with

$$\Delta Z := \frac{\delta E(Z) - \delta E(Z-1)}{FWHM}$$

- ■ CLTD + Si_3N_4 (present data)
- ♦ CLTD + Si_3N_4 (test at Garching)
- ○ IC + Parylene-C (Quade et al.)
- △ IC + Parylene-C (prediction by Bocquet et al.

substantial improvement for heavy masses due to:

⇒ energy resolution

⇒ energy linearity (no pulse hight defect)

⇒ no entrance window

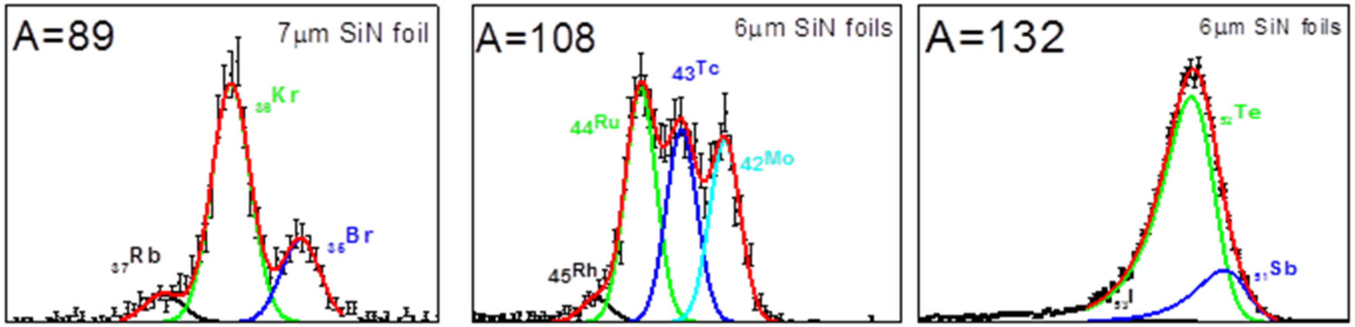

Procedure for Determining Accurate Absolute Z-Yields

- fit of spectrum
  - ⇒ relative Z-Yield
  - ⇒ line shape from Tandem experiment (one single Z)

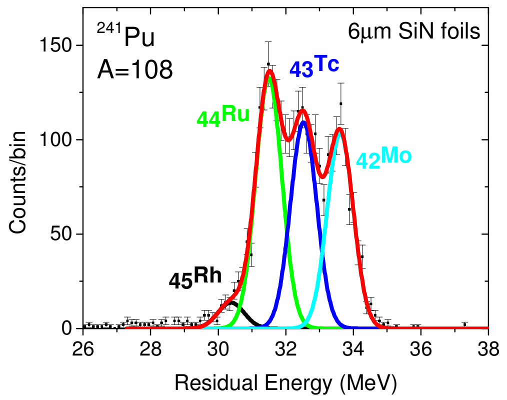

Procedure for Determining Accurate Absolute Z-Yields

- fit of spectrum
  - ⇒ relative Z-Yield
  - ⇒ line shape from Tandem experiment (one single Z)
- Z-Identification

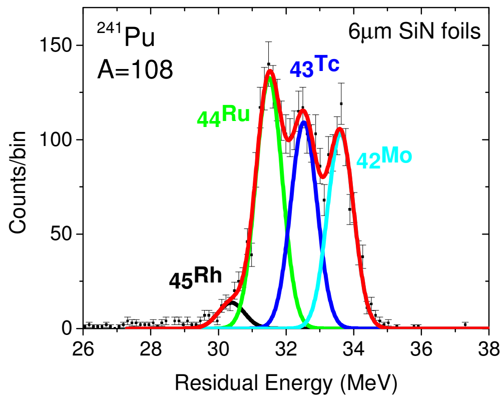

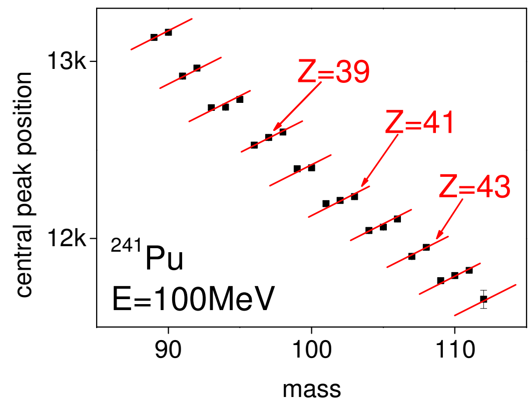

Procedure for Determining Accurate Absolute Z-Yields

- fit of spectrum
  - ⇒ relative Z-Yield
  - ⇒ line shape from Tandem experiment (one single Z)
- Z-Identification
- take into account
  - ⇒ energy dependence

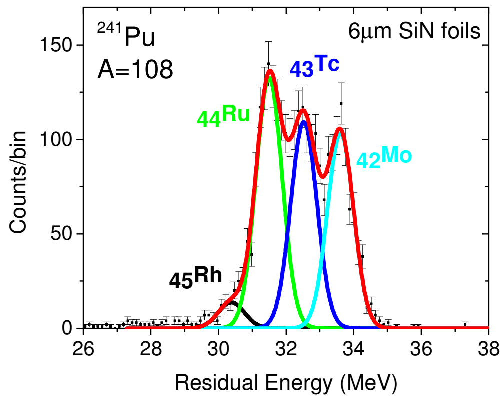

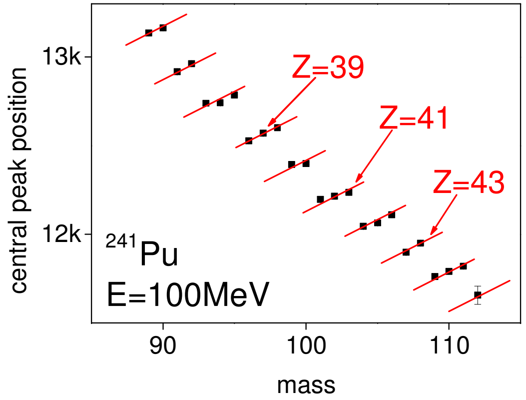

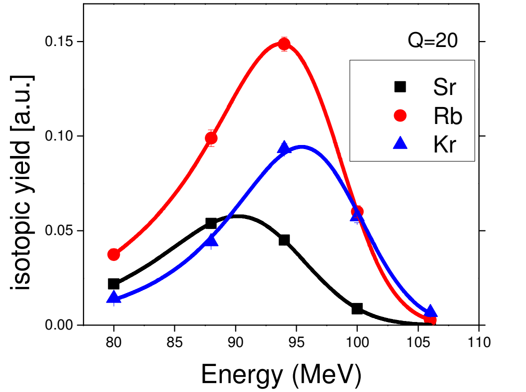

Procedure for Determining Accurate Absolute Z-Yields

- fit of spectrum
  - ⇒ relative Z-Yield
  - ⇒ line shape from Tandem experiment (one single Z)
- Z-Identification
- take into account
  - ⇒ energy dependence
  - ⇒ electronic charge state dependence (isomeric states)

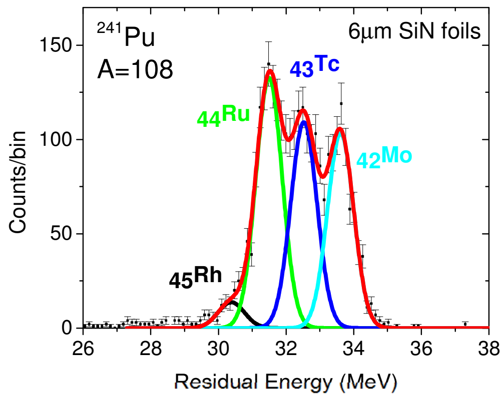

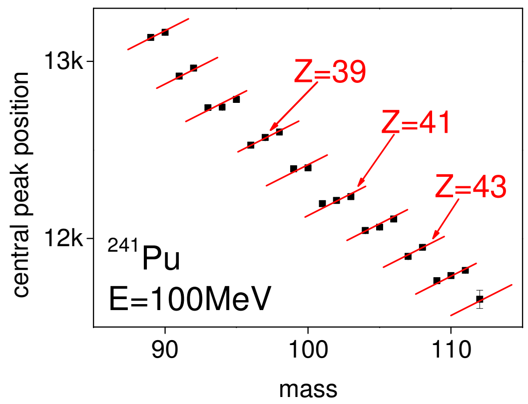

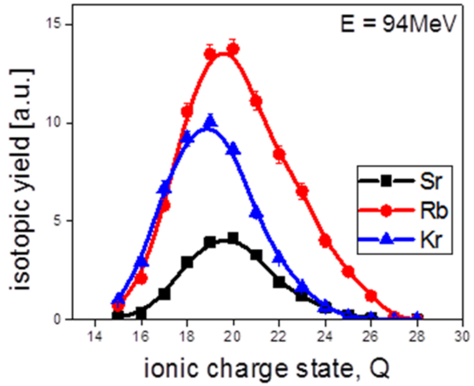

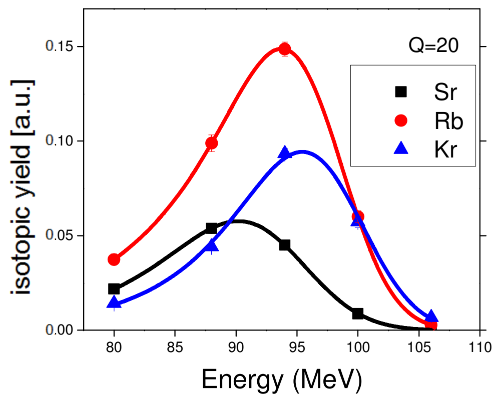

Procedure for Determining Accurate Absolute Z-Yields

- fit of spectrum
  - ⇒ relative Z-Yield
  - ⇒ line shape from Tandem experiment (one single Z)
- Z-Identification

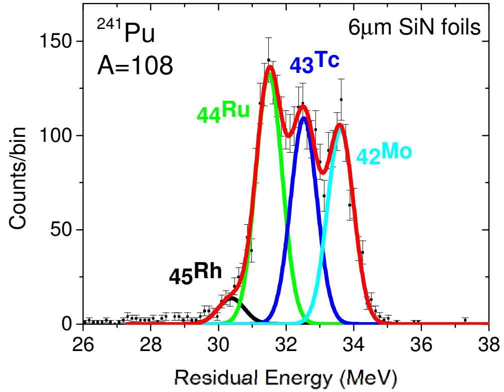

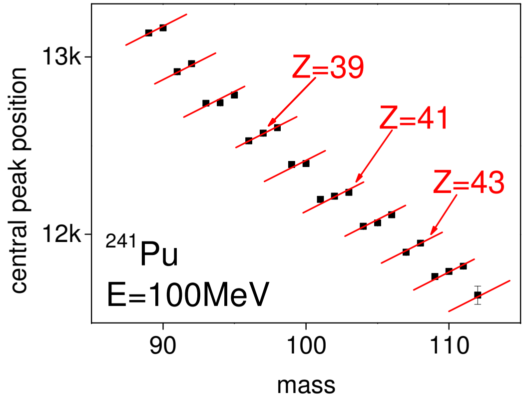

- take into account
  - ⇒ energy dependence
  - ⇒ electronic charge state dependence (isomeric states)

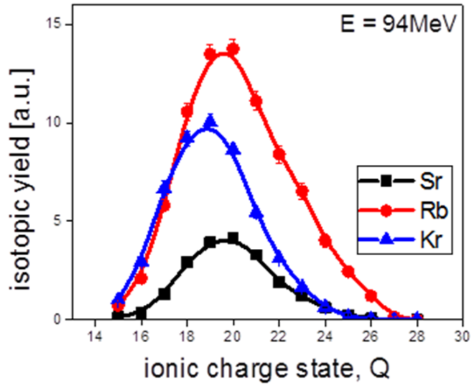

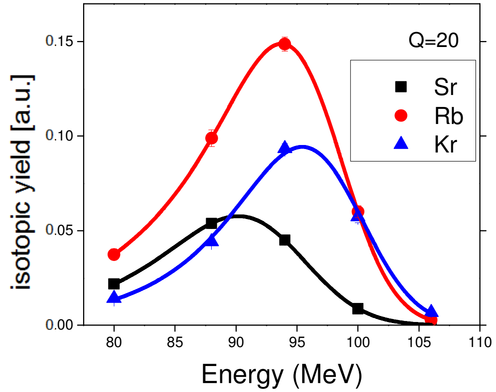

- absolute normalization
  - ⇒ target burnup

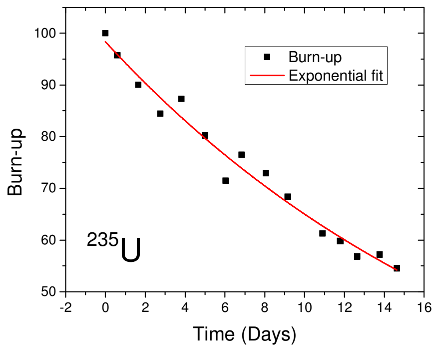

Procedure for Determining Accurate Absolute Z-Yields

- fit of spectrum
  - ⇒ relative Z-Yield
  - ⇒ line shape from Tandem experiment (one single Z)
- Z-Identification

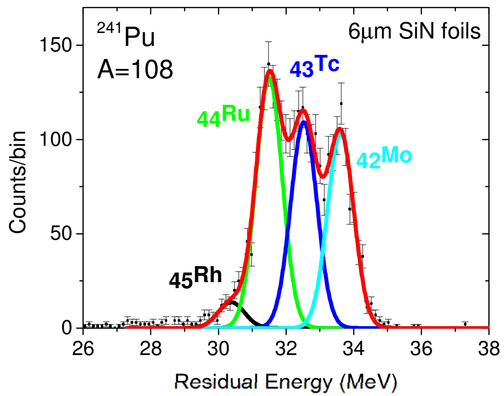

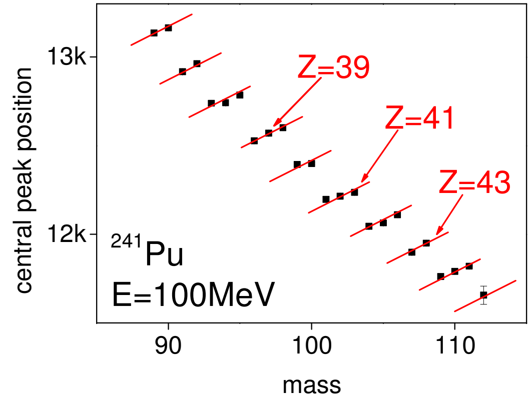

- take into account
  - ⇒ energy dependence
  - ⇒ electronic charge state dependence (isomeric states)

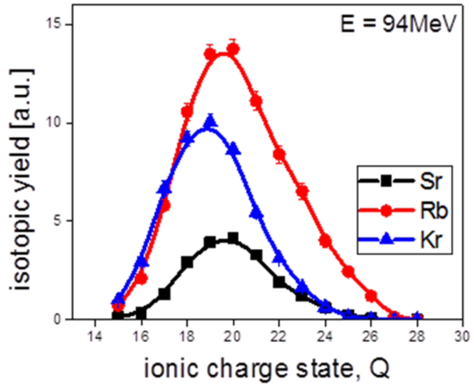

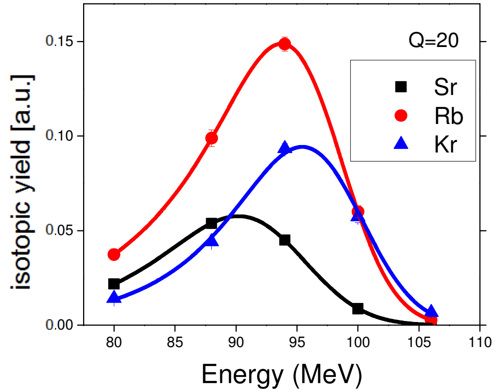

- absolute normalization
  - ⇒ target burnup

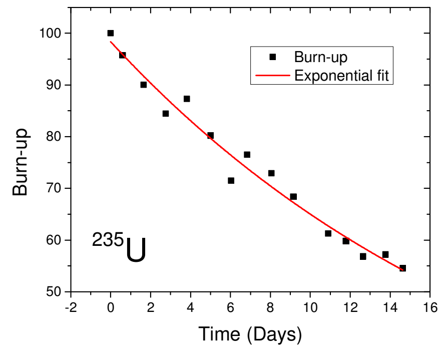

for Z-Yield for one mass:

⇒ about 300 spectra to be analyzed

Results on ^{92}Rb

Motivation for investigating Mass 92: The Reactor Antineutrino Anomaly

⇒ 5.7% deficit of measured antineutrinos
as expected from β-decay data of fission fragments

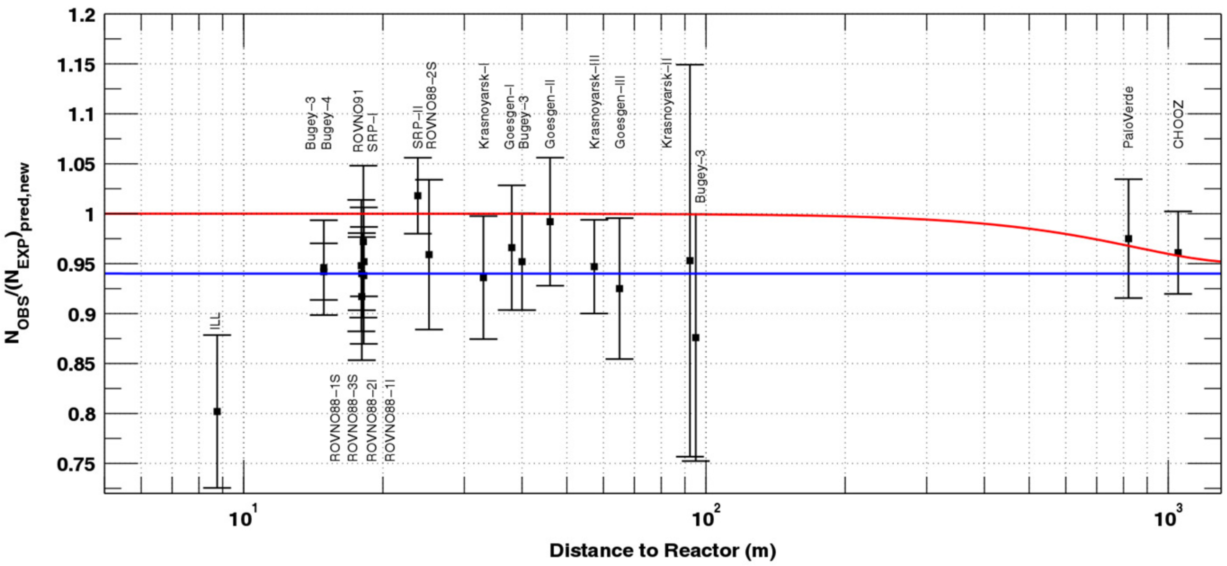

G. Mention et al., Phys. Rev. D83 (2011) 073006

possible explanations: ⇒ 4th non standard „sterile" neutrino
⇒ wrong Z-yields of fission fragments

Results: Mass 92

Motivation:

PHYSICAL REVIEW C **91**, 011301(R) (2015)

Nuclear structure insights into reactor antineutrino spectra

A. A. Sonzogni, T. D. Johnson, and E. A. McCutchan
National Nuclear Data Center, Brookhaven National Laboratory, Upton, New York 11973-5000, USA

(Received 8 August 2014; revised manuscript received 25 November 2014; published 8 January 2015)

Antineutrino spectra following the neutron induced fission of ^{235}U, ^{238}U, ^{239}Pu, and ^{241}Pu are calculated using the summation approach. While each system involves the decay of more than 800 fission products, the energy region of the spectra most relevant to neutrino oscillations and the reactor antineutrino anomaly is dominated by fewer than 20 nuclei, for which we provide a priority list to drive new measurements. The very-high-energy portion of the spectrum is mainly due to the decay of just two nuclides, ^{92}Rb and ^{96}Y. The integral of the signal measured by antineutrino experiments is found to have a dependence on the mass and proton numbers of the fissioning system. In addition, we observe that ~70% of the signal originates from the light fission fragment group and about 50% from the decay of odd-Z, odd-N nuclides.

The ^{92}Rb cumulative fission yield following the thermal fission of ^{235}U definitely merits a new measurement. While

Results on ^{92}Rb

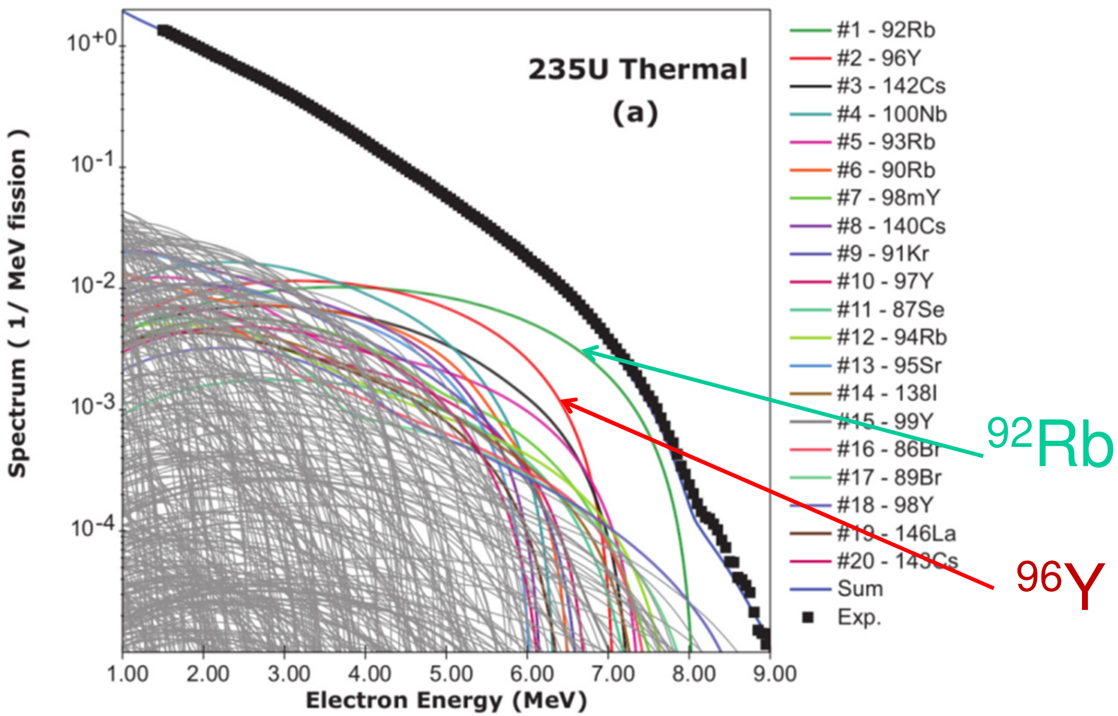

A. A. Sonzogni et al., Phys. Rev. C91 (2015) 011301 (R)

TABLE III. Same as Table II, except the strongest contributors from ^{235}U at 5.5 MeV are summarized.

Nuclide	Q_β (MeV)	GS BR (%)	$J^\pi_{gs} \rightarrow J^\pi_{gs}$	Contr. (%)
^{92}Rb	8.1	95.2(7)	$0^- \rightarrow 0^+$	21.6
^{96}Y	7.1	95.5(5)	$0^- \rightarrow 0^+$	14.5
^{142}Cs	7.3	56(5)	$0^- \rightarrow 0^+$	6.8
^{100}Nb	6.4	50(7)	$1^+ \rightarrow 0^+$	4.7
^{93}Rb	7.5	35(3)	$5/2^- \rightarrow 7/2^+$	4.6
^{90}Rb	6.6	33(4)	$0^- \rightarrow 0^+$	3.4
^{98m}Y	9.0	12(5)[a]	$(4,5) \rightarrow 4^+$	2.8
^{140}Cs	6.2	36(2)	$1^- \rightarrow 0^+$	2.4
^{91}Kr	6.8	18(3)[b]	$5/2^{(+)} \rightarrow (5/2^-)$	2.4

[a]Strongest branch to a low-lying state is to a 4^+, 1843-keV level.
[b]Strongest branch is to a $(5/2^-)$, 109-keV level.

for ^{235}U target: contribution of ^{92}Rb to the β-spectrum at 5.5 MeV

⇒ JEFF data basis: 21.6%

⇒ Tipnis et al. 30.0%

A. A. Sonzogni et al.:

The ^{92}Rb cumulative fission yield following the thermal fission of ^{235}U definitely merits a new measurement.

Results on ^{92}Rb for ^{235}U Target

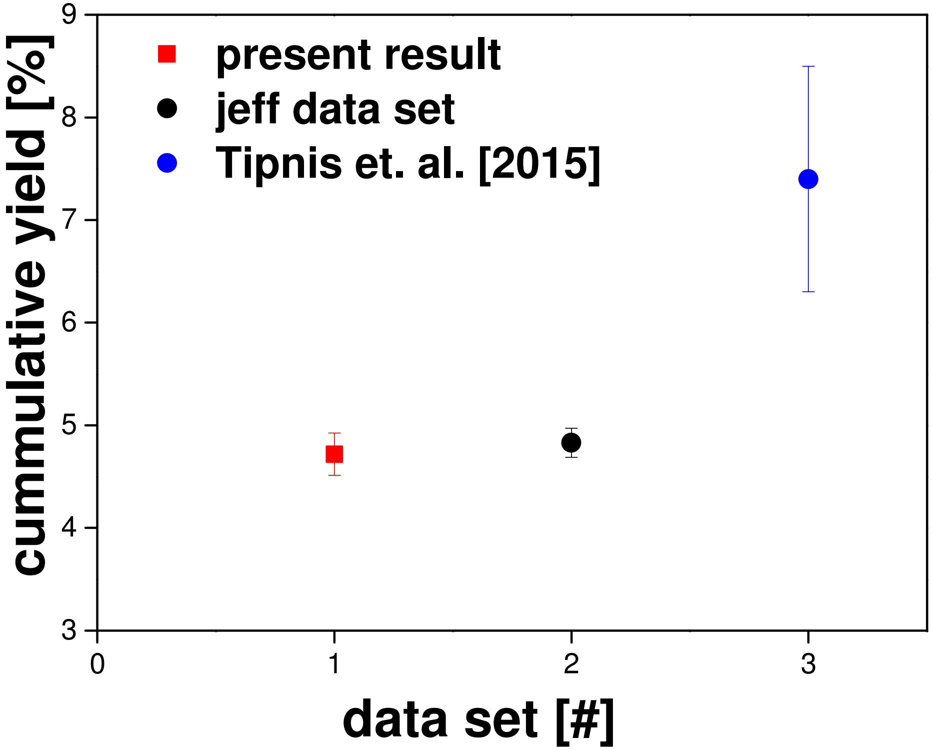

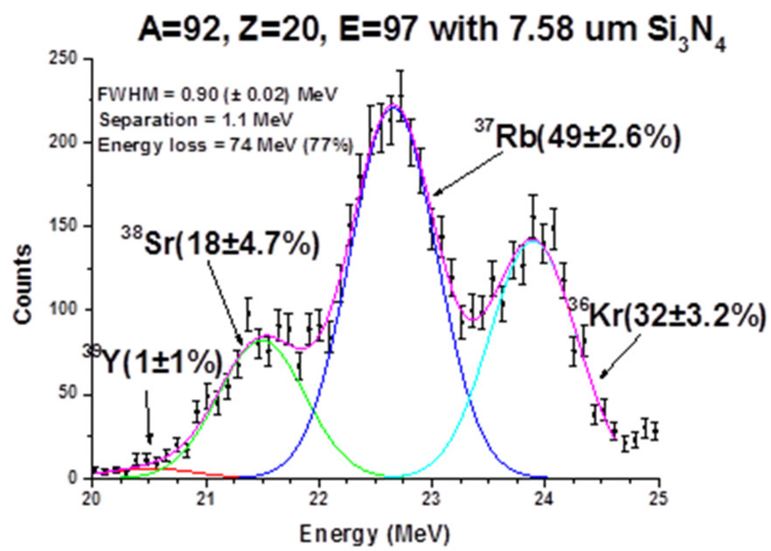

JEFF Report: M.A. Kellett et al., Nucl. Energy Agency, OECD,2009
S.V. Tipnis et al., Phys. Rev. C58 (1998) 905

^{92}Rb data for ^{239}Pu and ^{241}Pu targets and
^{96}Y data for all 3 targets to be analysed

Results on ^{241}Pu covering the Symmetry Region: Mean Z

mean nuclear charge <Z>

deviation from "democratic" distribution of neutron excess
Z_{UCD} - <Z> , Z_{UCD} = 94/242 X A

symmetry region

Z_{heavy} = 50

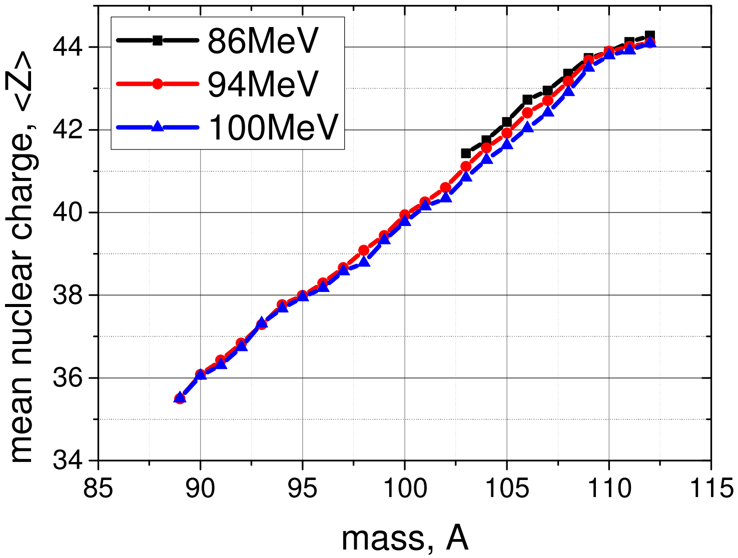

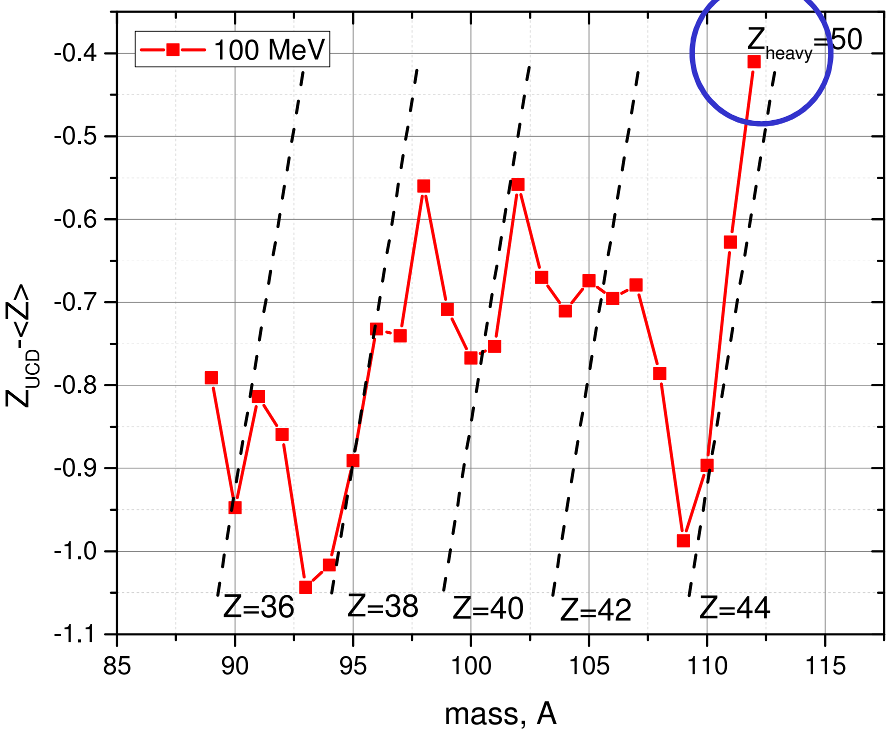

data preliminary

Results on ^{241}Pu covering the Symmetry Region: Z Yields

Motivation:

⇒ How behaves the even-odd staggering in the transition to the symmetry region?

⇒ Is there a change in the fission mode?

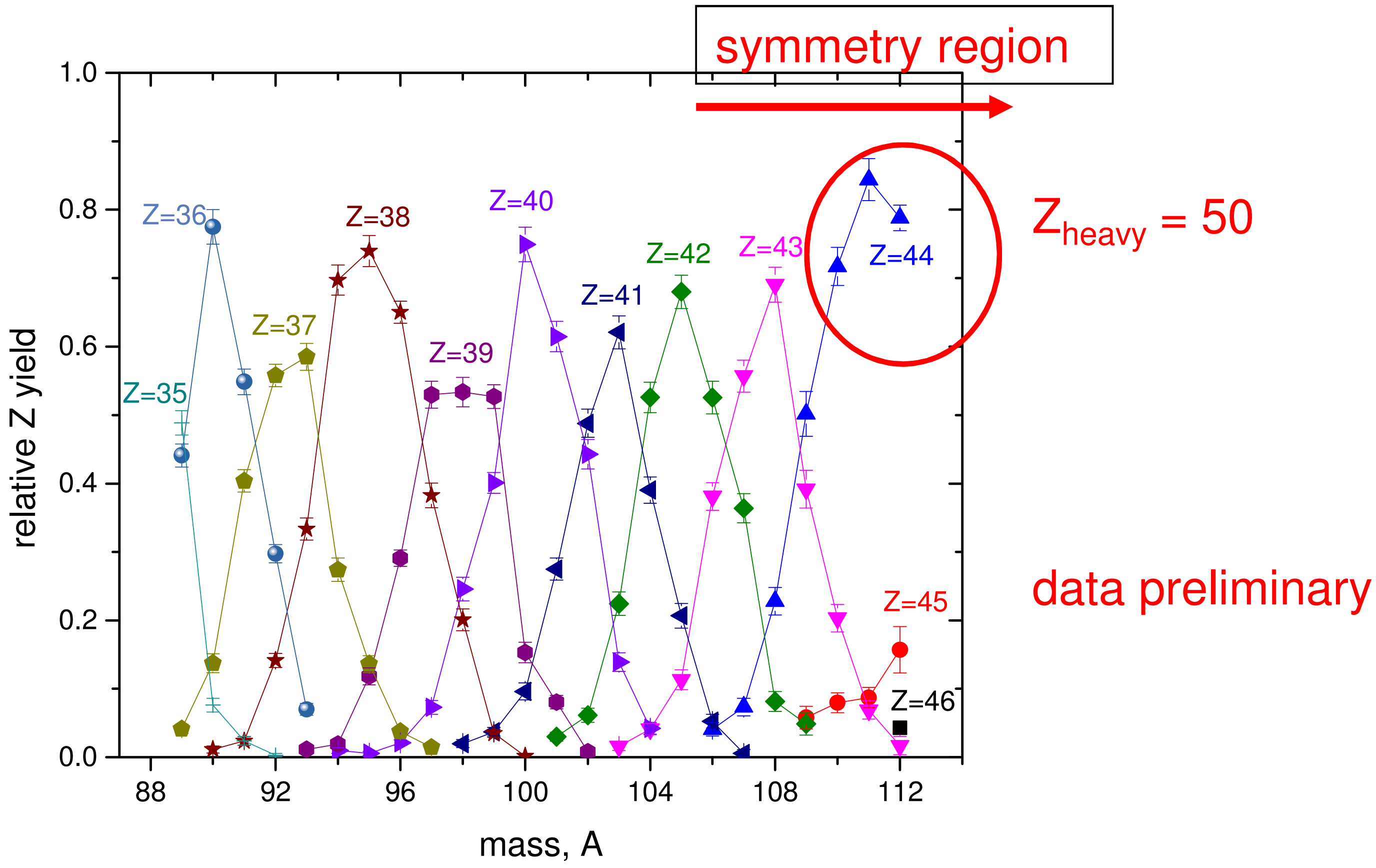

data for ^{239}Pu target in the symmetry region to be analysed

Collaboration

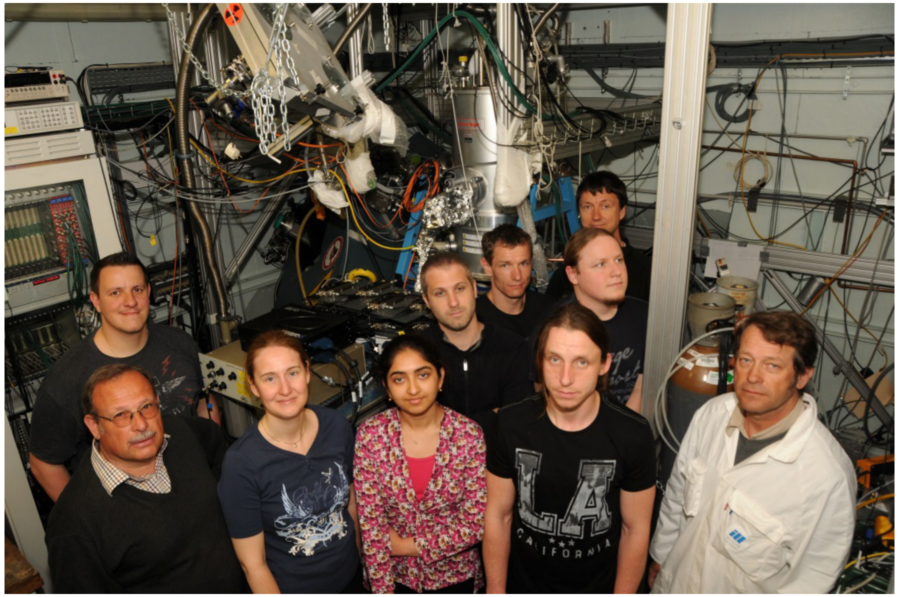

Santwana Dubey[1,2], Victor Andrianov[3] Shawn Bishop[4], Aurelin Blanc[6], Artur Echler[1,2,3], Peter Egelhof[1,2], Herbert Faust[6] , Friedrich Gönnenwein[5], Patrick Grabitz[1,2], Jose Gomez[4], Ulli Köster[6], Saskia Kraft-Bermuth[3], Werner Lauterfeld[2], Manfred Mutterer[5], Pascal Scholz[3], S. Stolte[2]

[1]GSI Helmholtzzentrum für Schwerionenforschung, Darmstadt, Germany
[2]Johannes Gutenberg Universität, Mainz, Germany
[3]Justus-Liebig-Universität, Gießen, Germany
[4]Technische Universität München, Germany
[5]Universität Tübingen, Germany
[6]Institut Laue-Langevin, Grenoble, France

V. Other Applications of CLTD`s in Heavy Ion Physics

- High Resolution Nuclear Spectroscopy
- Investigation of Stopping Powers of Heavy Ions in Matter
- In-Flight Mass Identification of Heavy Ions by E-TOF
- Accelerator Mass Spectrometry
- Lamb Shift Measurements in Hydrogen-Like Heavy Ions
- Investigation of Z-Yield Distributions of Fission Fragments

Applications:
a) High Resolution Nuclear Spectroscopy

nuclear spectroscopy:

- elastic and inelastic scattering ⇒ separation of inelastic channels
- nuclear reactions ⇒ identification of reaction channels

Example:

investigation of giant resonances
(collective excitation of nuclear matter)

J. Meier et al.
Nucl. Phys. A 626 (1997) 451c

^{Nat}Pb (^{20}Ne, $^{20}Ne'$), E = 100 MeV/u
(CLTD adjusted to range of Ne ions)

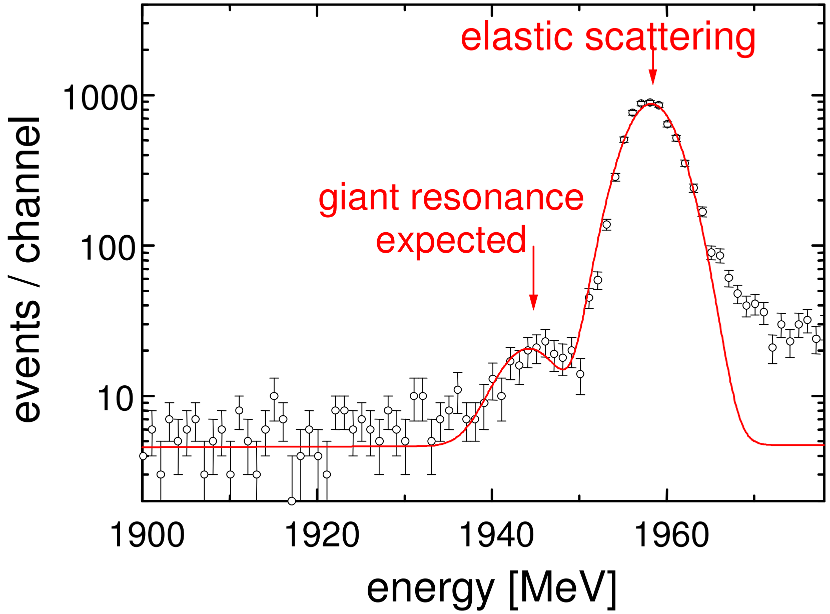

potential applications:

⇒ investigation of multi phonon giant resonances
⇒ reactions at low energies (LEB at FAIR)

Applications:
b) Investigation of Stopping Powers of Heavy Ions in Matter

motivation:

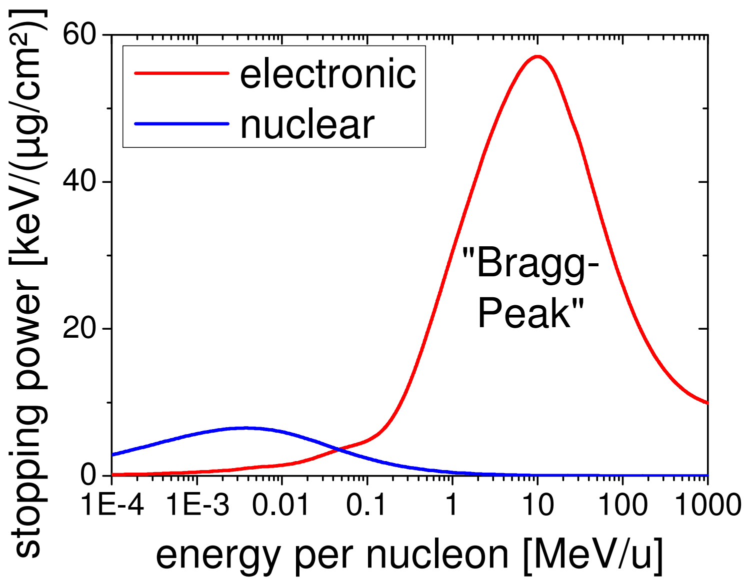

example: stopping power of ^{238}U-ions in gold (SRIM-prediction)

energy loss processes:

- electronic stopping power
  = ionization of target atoms
- nuclear stopping power
  = elastic scattering on target nuclei

important: theoretical understanding

- basic science:
  - interaction of energetic particles with matter
- applied science:
  - material science
  - investigation of radiation damage
  - medicine → tumor therapy
  - …

problem:

accuracy of theoretical models unsatisfactory

⇒ predictions by semi-empirical computer codes

- use best fits on experimental data (example: SRIM)

⇒ many data needed for different kind of

- targets, projectiles, energies

in particular:

data for very slow and very heavy ions are still scarce

The TOF – CLTD Spectrometer
- A New Experimental Method for dE/dx Measurements

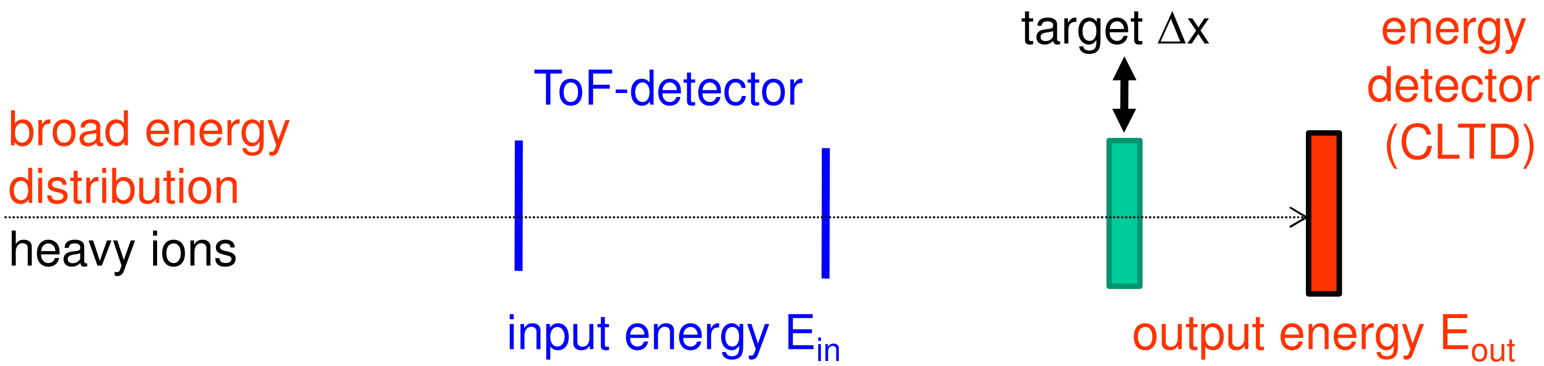

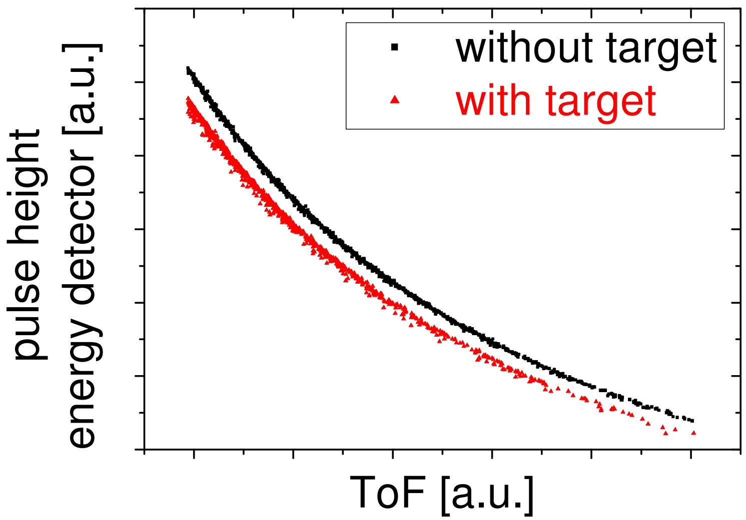

as compared to previous measurements with conventional energy detector

(for example: Trzaska et al., Zhang et al.):

$\Rightarrow$ by use of CLTD's as energy detector:

- improved energy resolution
  $\rightarrow$ higher sensitivity
- improved energy linearity
  (no pulse height defect)
  $\rightarrow$ reduced energy calibration errors

Stopping Power Measurements at GSI and JYFL

UNILAC accelerator (GSI, Darmstadt)
0.1 – 1.4 MeV/u ^{238}U ions in C- und Au-targets

K-130 cyclotron (JYFL, Jyväskylä)
0.05 – 1 MeV/u ^{131}Xe ions in C-, Ni- und Au-targets

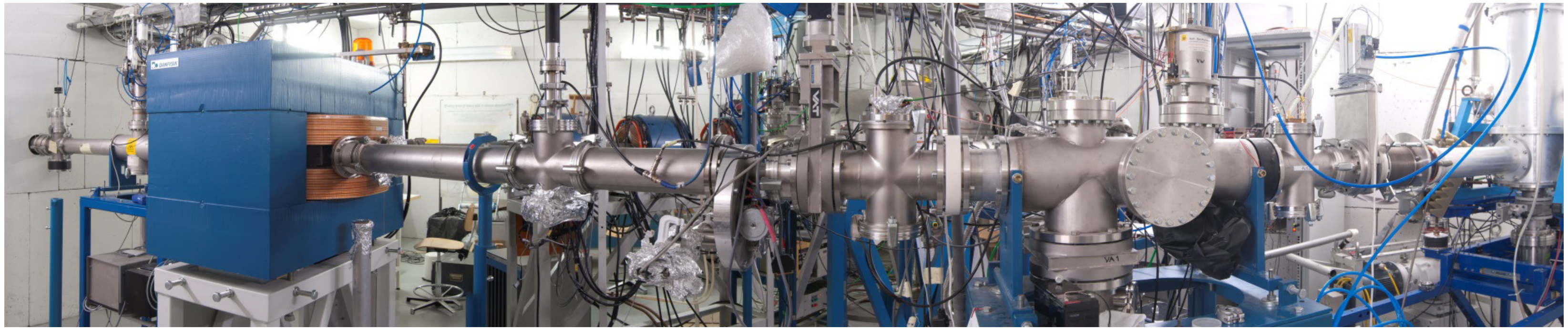

Results on Stopping Powers for ^{131}Xe-Ions in C, Ni and Au

measurements JYFL Jyväskylä in cooperation with H. Kettunen, W. Trazka et al.

experimental setup:

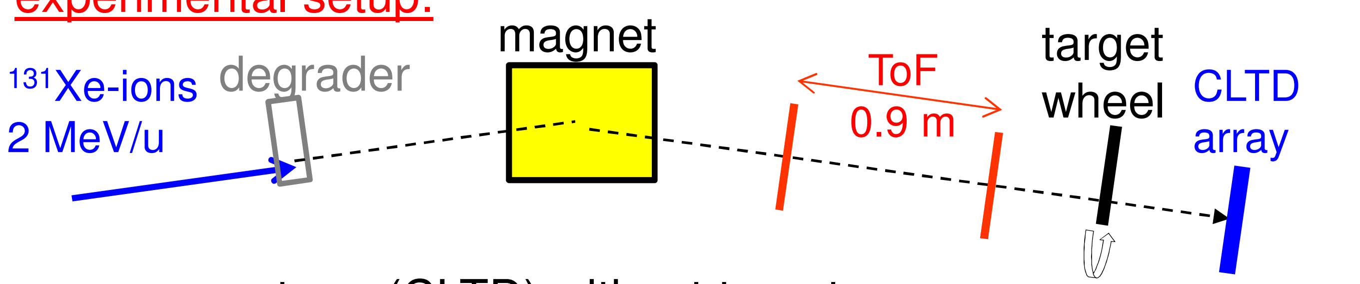

target thickness Δx determined by weighting + energy loss of α-particles
→ high accuracy

energy spectrum (CLTD) without target

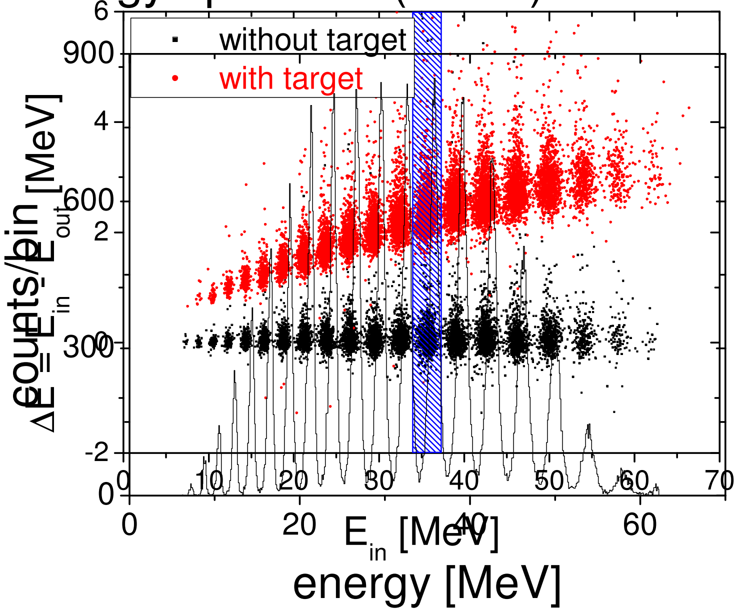

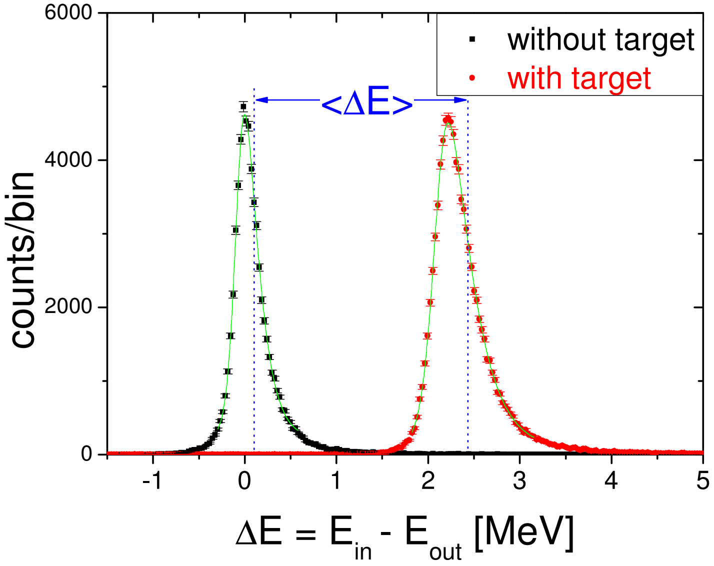

structure in energy distribution due to charge state selection in the magnet

example: ^{131}Xe in 53 µg/cm^2 carbon

Results on Stopping Powers: 0.05 – 1.0 MeV/u ^{131}Xe-Ions in C

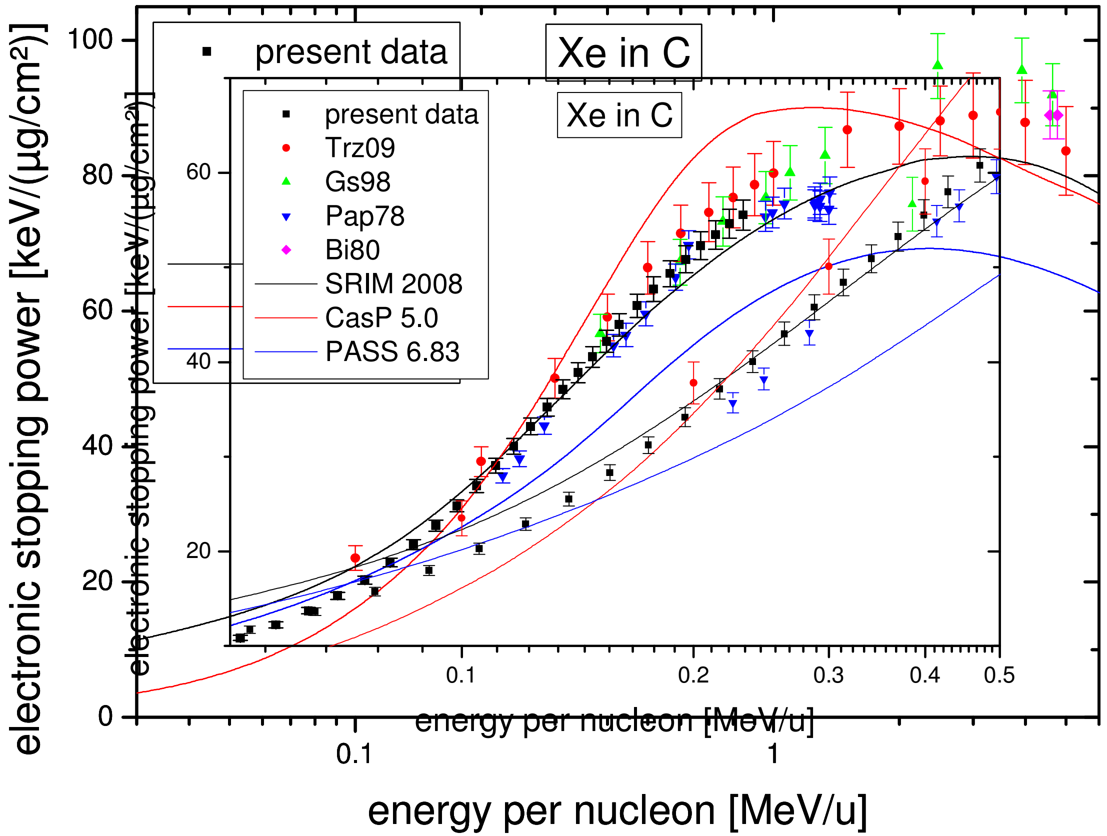

reference data taken from online database of H. Paul:
http://www.exphys.jku.at/stopping/

A. Echler, PHD thesis 2013

and A. Echler et al. Nucl. Instr. Meth. B391 (2017) 38

- substantial deviations from SRIM-predictions (semiempirical calculations)

experimental uncertainties:

- detector-cal.: <1 %
- target foils: 3 %
- statistics: <0.5 %
  (lowest energies: <2 %)
- **total: 3 – 4 %**

(improvement of factor 2-3)

- agreement with Geissel et al.
- deviations from data from Trzaska et al. and Pape et al.
- data extended to lower energies

Stopping Power Measurements – Effect of Channeling: Xe in Au

for thin Ni- and Au-targets:
→ double-peak structure in measured energy loss

explanation:

“channeling energy loss” “random energy loss”

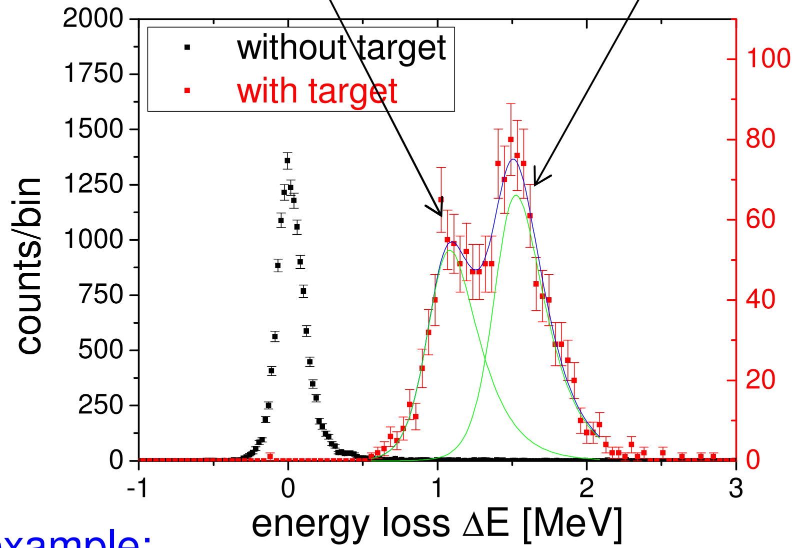

example:
Xe (13 – 15 MeV) in Au (363 μg/cm²)

A. Echler, PHD thesis 2013
and
A. Echler et al.,
Nucl. Instr. Meth. B391 (2017) 38

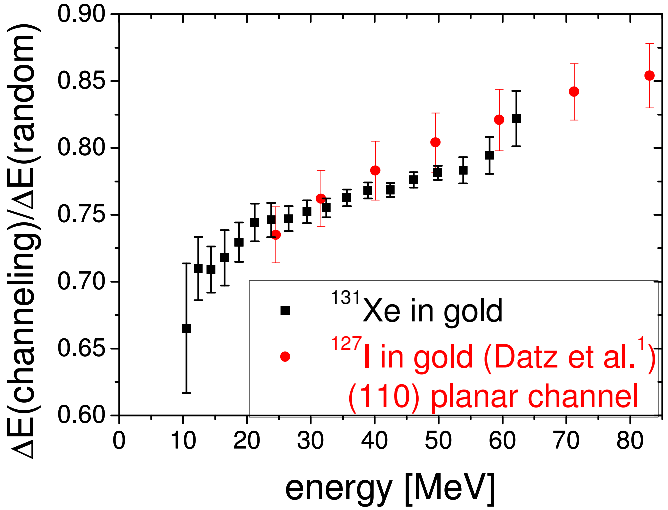

1)Datz et al., Nucl. Inst. Meth., 38 (1965) 221

⇒ new data on channeling energy loss obtained
⇒ source of systematic error identified and eliminated

X-Ray Diffraction Analysis of the Absorber Foils

Is the interpretation of the data correct? channeling appears only in crystalline absorbers!
problem: targets not grown as single crystals

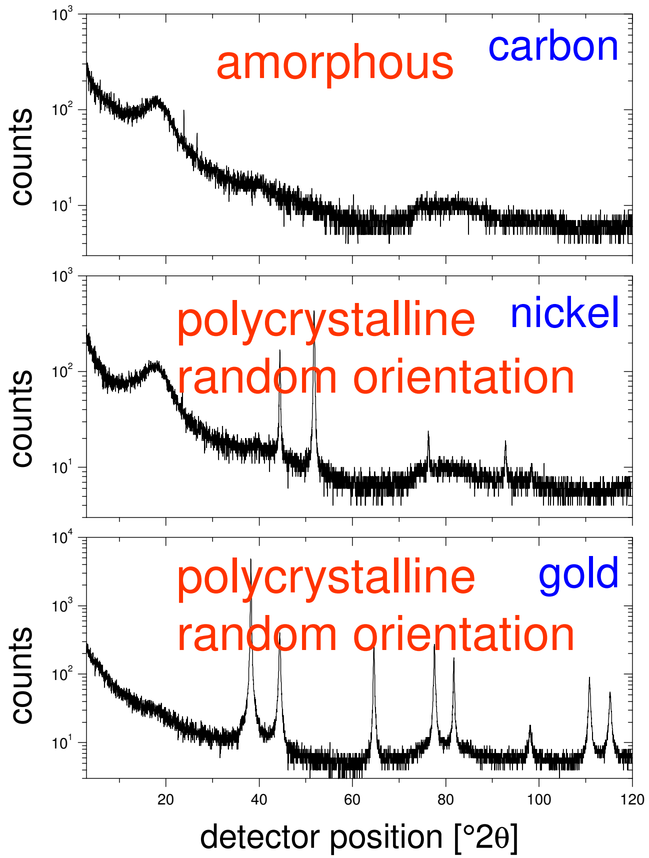

the X-ray analysis confirms polycrystalline structure in Ni and Au foils

the channeling effect is enhanced due to much stronger multiple scattering for random energy loss

Results on Stopping Powers: 0.09 – 1.0 MeV/u ^{131}Xe-Ions in Ni (only Random Energy Loss)

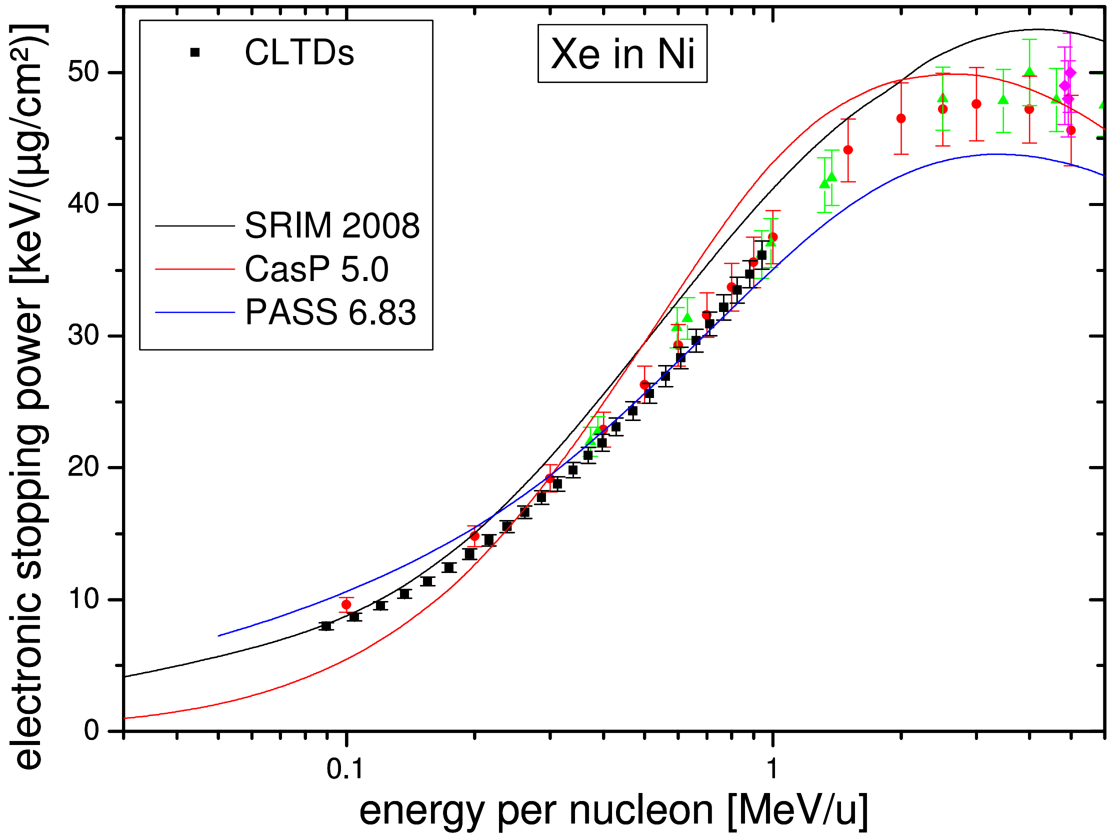

experimental uncertainties:

- detectorcal.: <1 %
- target foils: 3 %
- statistics: <1 %
  (lowest energies: <2 %)
- total: 3 – 4 %

➢ substantial deviations from SRIM-predictions

➢ agreement with Geissel et al.

➢ deviations from data of Trzaska et al. for low energies

reference data taken from online database of H. Paul:
http://www.exphys.jku.at/stopping/

Perspectives for further Applications

- Investigation of Heavy Ion Channeling in Single Crystals (A. Bräuning- Demian et al., C. Trautmann et al.)

- Investigation of Charge Exchange Energy Straggling (proposed by H. Geissel et al.)

Applications:
c) In-Flight Mass Identification of Heavy Ions

important for many applications: isotope mass identification

standard method:

$B \bullet \rho \Rightarrow p$
TOF $\Rightarrow v$

$$m = \frac{p}{v}$$

disadvantage:

- needs big magnet spectrometer
- small solid angle
- charge state ambiguity because of $B \bullet \rho = p/Q$ (especially for slow heavy ions!)
- small dynamic range

alternative method:

energy $\Rightarrow E$
TOF $\Rightarrow v$

$$m = \frac{2E}{v^2}$$

$$\left(\frac{\Delta m}{m}\right)^2 = \left(\frac{\Delta E}{E}\right)^2 + \left(2\frac{\Delta t}{t}\right)^2$$

for conventional setups: mass resolution is limited by energy resolution!
$\Rightarrow$ calorimetric detectors

In-Flight Mass Identification

measured at Tandem accelerator at MPI in Heidelberg

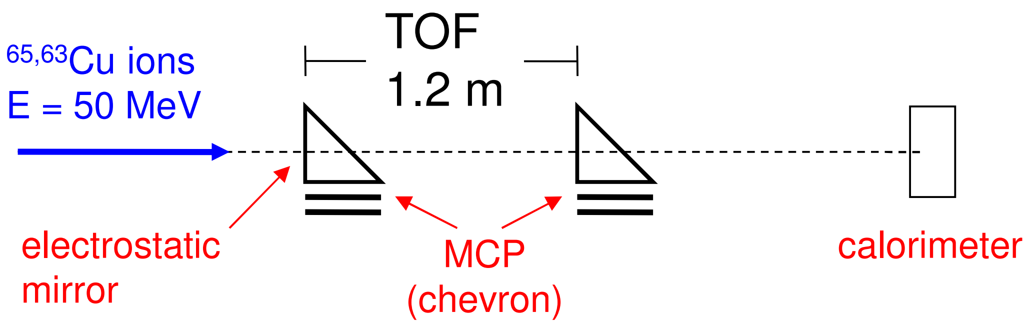

energy $\Rightarrow$ E
TOF $\Rightarrow$ v

$$m = \frac{2E}{v^2}$$

$$\left(\frac{\Delta m}{m}\right)^2 = \left(\frac{\Delta E}{E}\right)^2 + \left(2\frac{\Delta t}{t}\right)^2$$

^{63,65}Cu ions @ 50 MeV

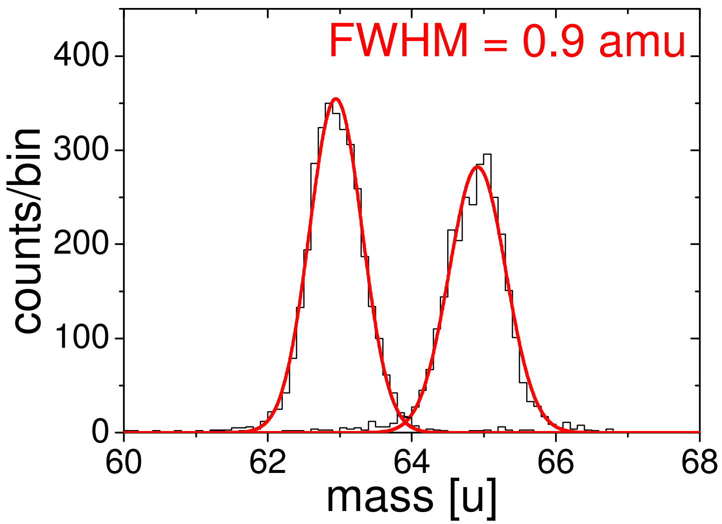

Δt = 680 ps

ΔE = 330 keV

limitation in this experiment:
TOF measurement !

A. Echler

PHD Thesis 2013

High Resolution In-Flight Mass Identification: Results for ^{131}Xe-Ions

low energetic ^{131}Xe ions @ K-130 cyclotron at JYFL Jyväskylä

experimental setup:

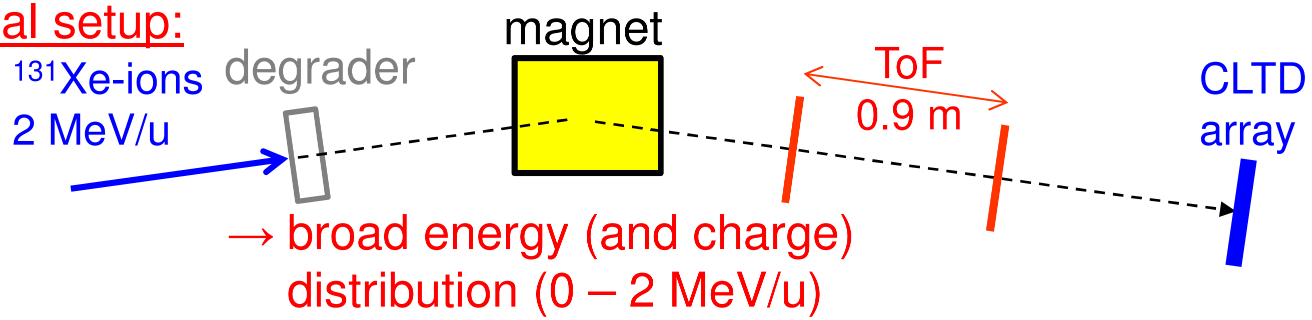

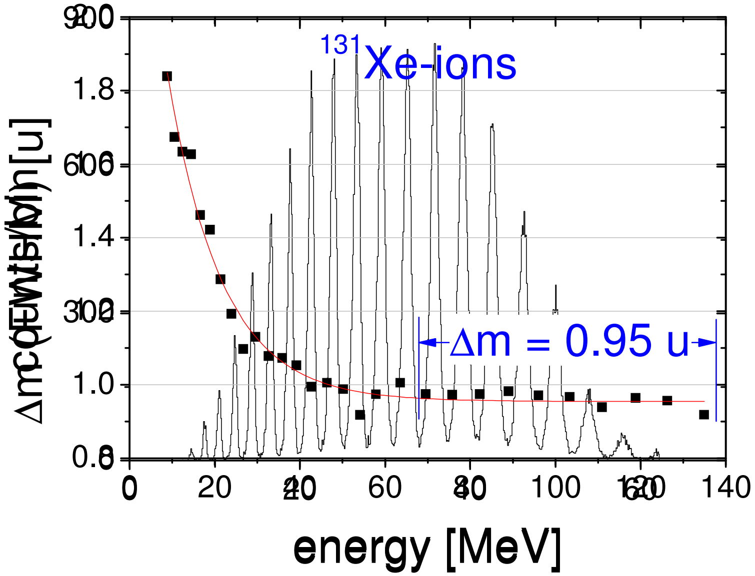

mass spectrum @ 107 – 115 MeV

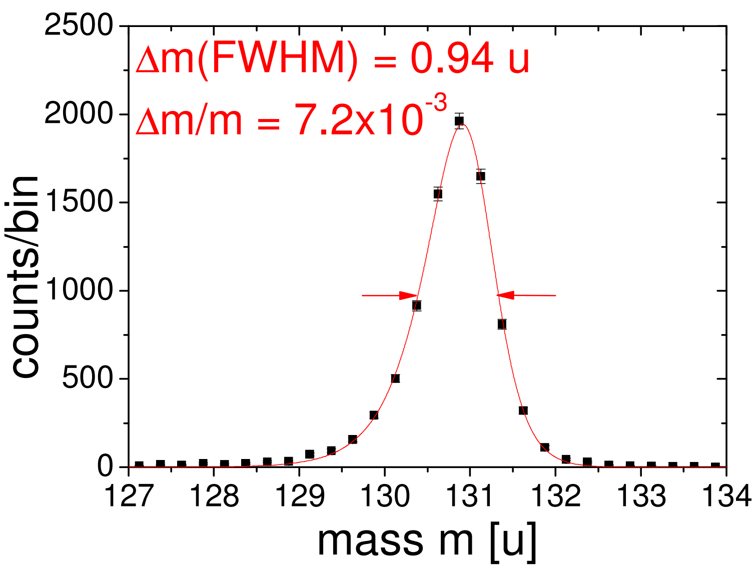

A. Echler, PHD Thesis 2013

In-Flight Mass Identification: Results for ^{238}U-Ions

experimental setup: low energetic ^{238}U ions @ UNILAC accelerator at GSI

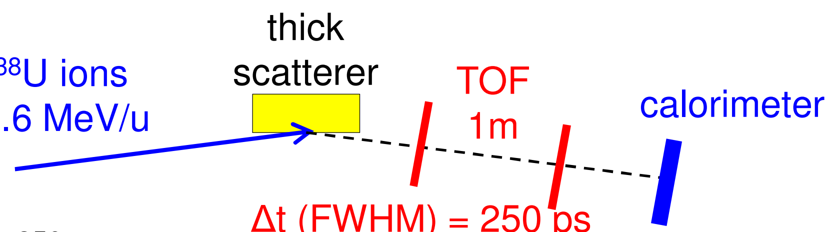

→ broad energy distribution
(0 - 3.6 MeV/u)

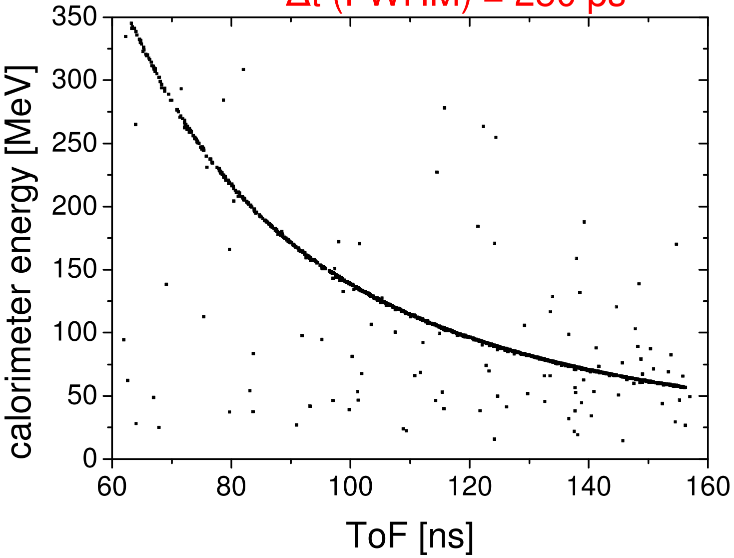

energy range: 65 - 150 MeV

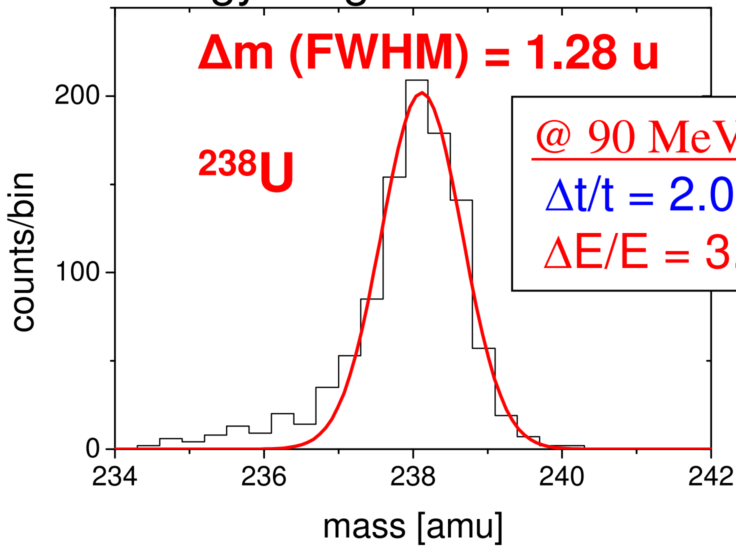

@ 90 MeV:
$\Delta t/t = 2.0 \times 10^{-3}$
$\Delta E/E = 3.5 \times 10^{-3}$

- not reachable with conventional E-ToF system
- advantage to Bρ-ToF method:
  - high dynamic range
  - not affected by charge state ambiguities

A. Echler, PHD Thesis 2013

Perspectives for Applications

In-Flight Mass Identification for:

- identification of reaction products from reactions with radioactive beams

(for slow heavy ions: no charge state ambiguities, high dynamic range)

⇒ potential application at NUSTAR@FAIR: LEB

⇒ investigation of deep inelastic transfer reactions (proposed by S. Heinz)

- identification of isotopes after in-flight gamma spectroscopy

⇒ potential application at NUSTAR@FAIR: HISPEC (LYCCA)

- identification of superheavy elements (for $Z \geq 113$: decay chain does not feed a known α-chain): $\Delta m \leq 1$ for $m = 300$ reachable

- identification of rare isotopes in accelerator mass spectrometry

⇒ high sensitivity

first experiment performed: trace analysis of 236U at the VERA facility at Vienna:
S. Kraft-Bermuth et al. Rev. Sci. Instr. 80 (2009) 103304

LYCCA Performance

transparency from J. Gerl

E-Tof mass identification: ΔA / A ≈ 1%
(presently limited to light mass region)

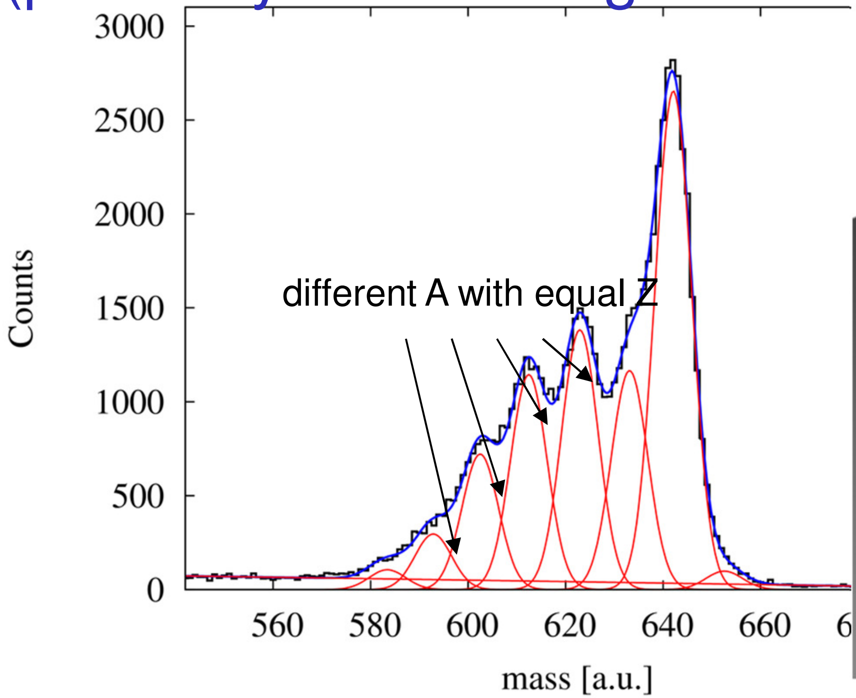

mass 56 - mass 66

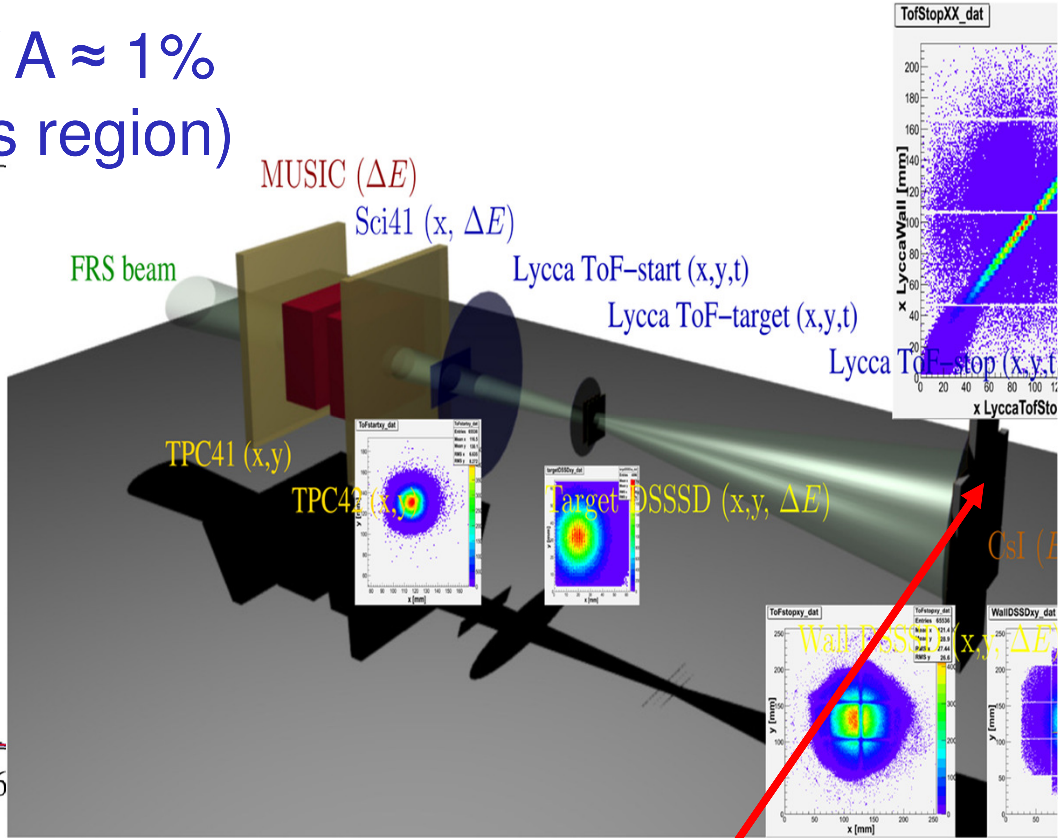

Idea:

replace CsI energy detector by a CLTD

Perspectives for Applications

In-Flight Mass Identification for:

- identification of reaction products from reactions with radioactive beams

(for slow heavy ions: no charge state ambiguities, high dynamic range)

$\Rightarrow$ potential application at NUSTAR@FAIR: LEB

$\Rightarrow$ investigation of deep inelastic transfer reactions (proposed by S. Heinz)

- identification of isotopes after in-flight gamma spectroscopy

$\Rightarrow$ potential application at NUSTAR@FAIR: HISPEC (LYCCA)

- identification of superheavy elements (for $Z \geq 113$: decay chain does not feed a known α-chain): $\Delta m \leq 1$ for $m = 300$ reachable

- identification of rare isotopes in accelerator mass spectrometry

$\Rightarrow$ high sensitivity

first experiment performed: trace analysis of 236U at the VERA facility at Vienna:

S. Kraft-Bermuth et al. Rev. Sci. Instr. 80 (2009) 103304

Identification of Superheavy Elements

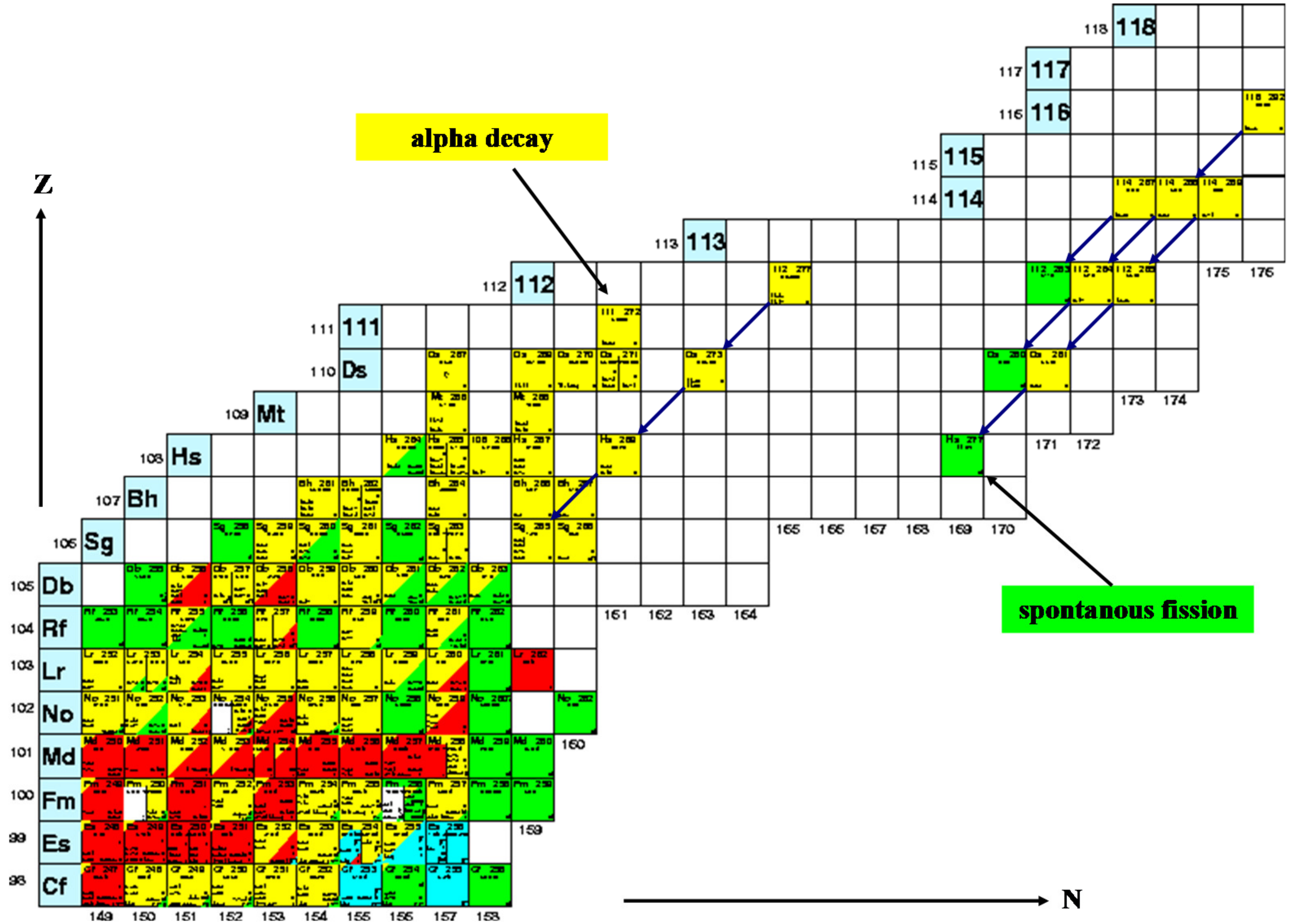

Application for Identification of Superheavy Elements

for Z ≥ 112: decay chains do not feed a known α-chain

⇒ mass identification of the superheavy nucleus required

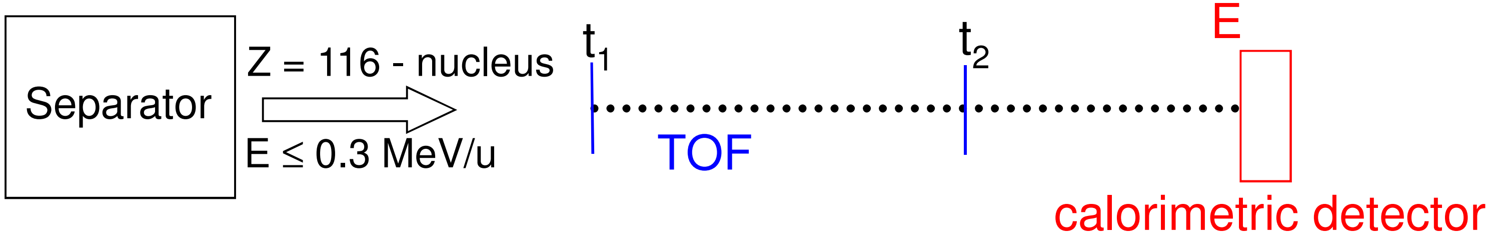

$$\left(\frac{\Delta m}{m}\right)^2 = 2\left(\frac{\Delta v}{v}\right)^2 + \left(\frac{\Delta E}{E}\right)^2$$

ultrathin ^{12}C-foils + channelplates

$$\frac{\Delta v}{v} \leq 1 \cdot 10^{-3}$$

(energy straggling in ^{12}C-foils negligible!)

calorimetric detector:

$$\frac{\Delta E}{E} \approx 2-3 \cdot 10^{-3}$$

(semiconductor detector: $\Delta E/E \geq 5 \bullet 10^{-2}$)

$$\frac{\Delta m}{m} \leq 3 \cdot 10^{-3}$$

for m = 300 ⇒ Δm ≤ 1 amu

First Test Experiment at SHIP

S. Kraft-Bermuth, PHD Thesis (2004)
(in cooperation with: D. Ackermann, F.Hessberger, S. Hofmann, G. Münzenberg)

reaction: ^{58}Ni + ^{102}Ru $\Rightarrow$ ^{160}Hf* $\Rightarrow$ $^{155(156)}$Yb + 2p +2(3)n

^{156}Yb $\xrightarrow{4.87\ \text{MeV}\ 20.8\ \text{s}}$ ^{152}Er $\xrightarrow{5.09\ \text{MeV}\ 8.4\ \text{s}}$ ^{148}Dy

^{156}Yb $\xrightarrow{4.92\ \text{MeV}\ 24.4\ \text{s}}$ ^{152}Er $\xrightarrow{4.89\ \text{MeV}\ 11.2\ \text{s}}$ ^{148}Dy

^{156}Yb $\xrightarrow{4.70\ \text{MeV}\ 36.4\ \text{s}}$ ^{152}Er $\xrightarrow{4.60\ \text{MeV}\ 11.6\ \text{s}}$ ^{148}Dy

literature: 4.69 MeV 26.1 s

literature: 4.80 MeV 10.3 s

^{155}Yb $\xrightarrow{5.44\ \text{MeV}\ 2.0\ \text{s}}$ ^{151}Er

^{155}Yb $\xrightarrow{5.33\ \text{MeV}\ 1.6\ \text{s}}$ ^{151}Er

^{155}Yb $\xrightarrow{5.35\ \text{MeV}\ 2.0\ \text{s}}$ ^{151}Er

literature: 5.20 MeV 1.8 s

$\Rightarrow$ **dynamic range sufficient to detect heavy ion and its α-decay time-resolved**

Perspectives for Applications

In-Flight Mass Identification for:

- identification of reaction products from reactions with radioactive beams

(for slow heavy ions: no charge state ambiguities, high dynamic range)

$\Rightarrow$ potential application at NUSTAR@FAIR: LEB

$\Rightarrow$ investigation of deep inelastic transfer reactions (proposed by S. Heinz)

- identification of isotopes after in-flight gamma spectroscopy

$\Rightarrow$ potential application at NUSTAR@FAIR: HISPEC (LYCCA)

- identification of superheavy elements (for $Z \geq 113$: decay chain does not feed a known α-chain): $\Delta m \leq 1$ for $m = 300$ reachable

- identification of rare isotopes in accelerator mass spectrometry

$\Rightarrow$ high sensitivity

first experiment performed: trace analysis of 236U at the VERA facility at Vienna:
S. Kraft-Bermuth et al. Rev. Sci. Instr. 80 (2009) 103304

Application of CLTD`s in Accelerator Mass Spectrometry (AMS)

application for Accelerator Mass Spectrometry:
(in collaboration with: R. Golser, W. Kutschera et al., VERA facility, Vienna)

aim: determination of very small isotope ratios $^{236}U/^{238}U$ in natural uranium samples
$\Rightarrow$ ^{236}U known as monitor for flux of thermal neutrons
(for example: investigation of Natural Reactors in Uranium Mines)

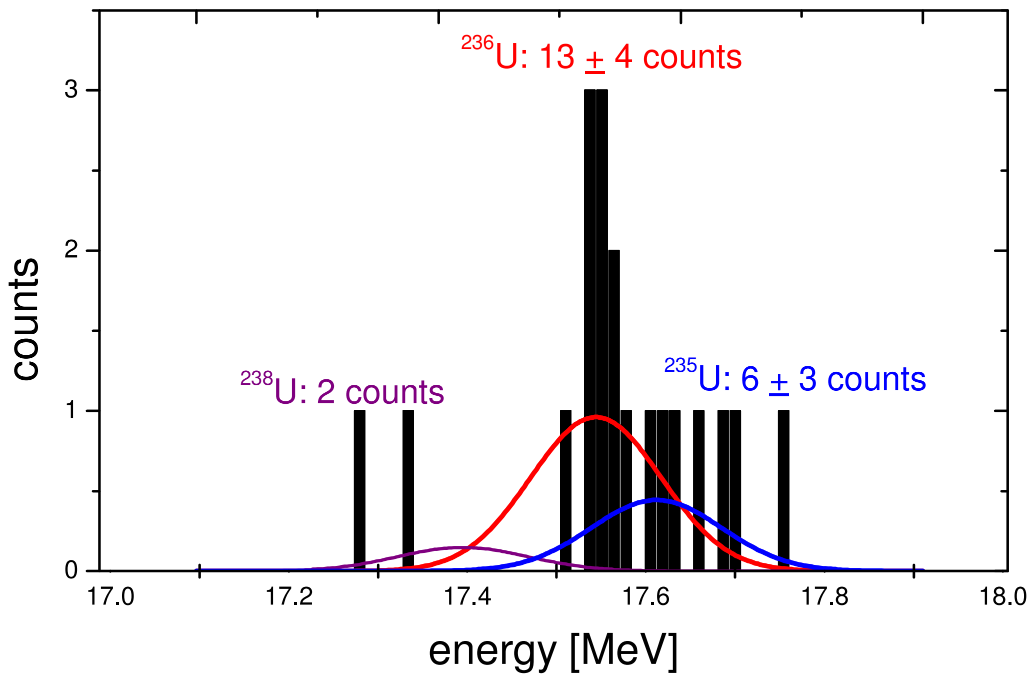

results:
substantial improvement in background discrimination and detection efficiency

$\Rightarrow$ level of sensitivity improved by one order of magnitude:

$$^{236}U/^{238}U = 7 \times 10^{-12}$$

S. Kraft-Bermuth et al.

Rev. Sci. Instr. 80 (2009) 103304

Other Applications in Heavy Ion Physics:
d) QED Tests by High Resolution X-Ray Spectroscopy

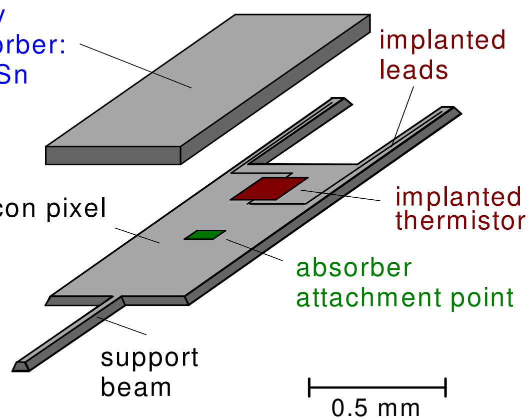

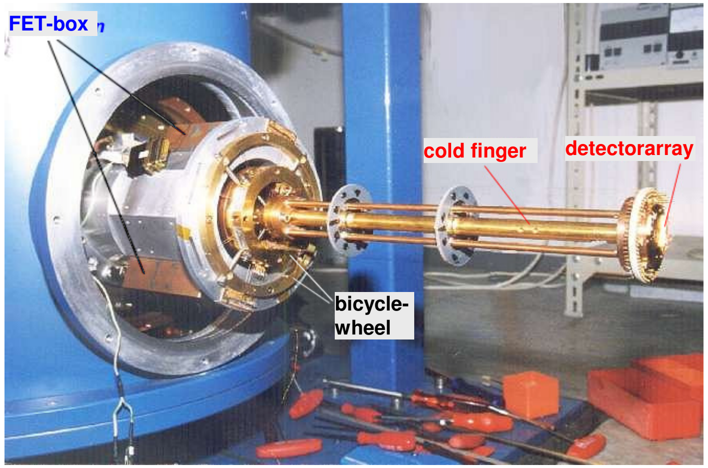

detection scheme:

- 36 pixel Si thermistors (from NASA/Goddard)
- Sn, Pb absorbers
- each pixel: $\approx 0.5\ \text{mm}^2 \times 85\ \mu\text{m}$
-- operated at 50 mK

detector performance:

- $\Delta E = 30 - 40$ eV @ 60 keV (theoretical limit of conventional Si detector: ≥ 350 eV)

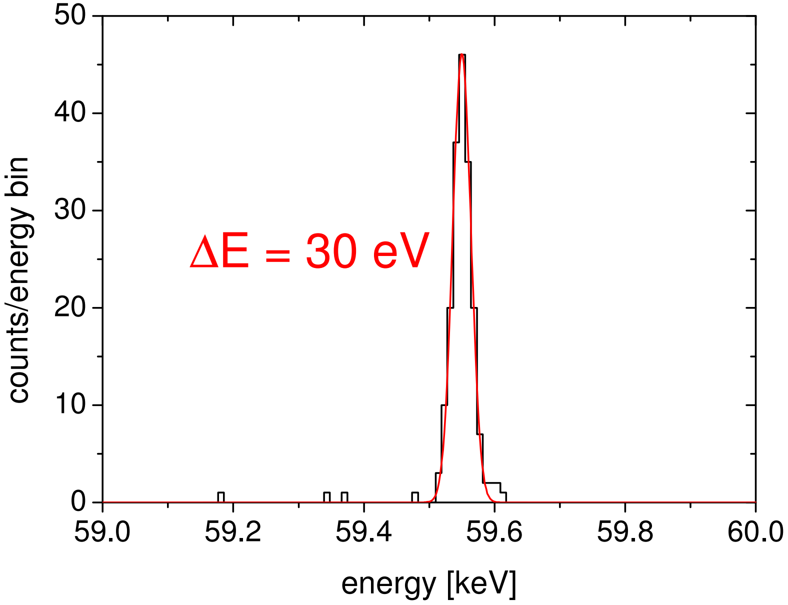

present status:

- detector with 24 pixels available
- active area: $10\ \text{mm}^2$

Perspectives: Test of QED in Extreme Static Electromagnetic Fields

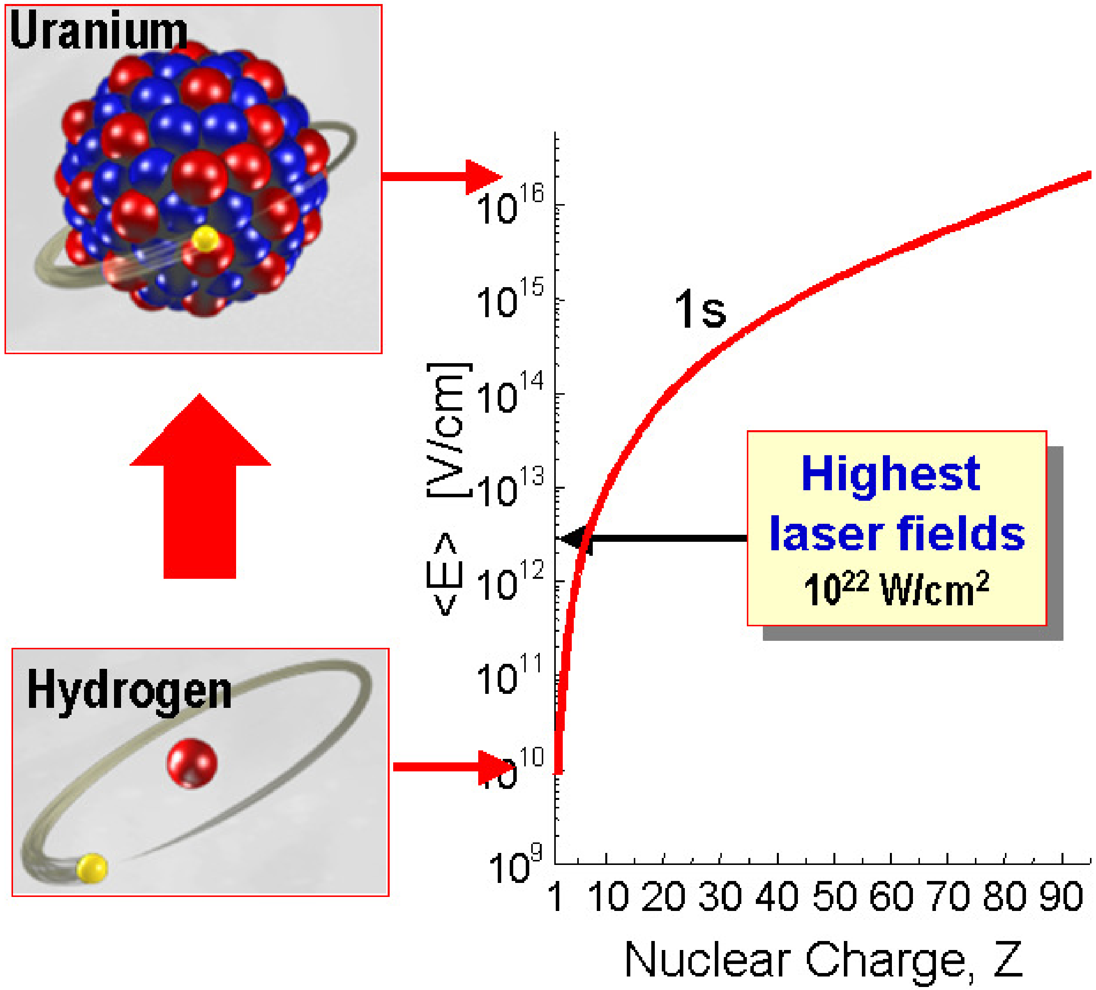

H-like Uranium
$\langle E \rangle = 1.8\times10^{16}$ V/cm
$E_K = -132\times10^{3}$ eV
$\Delta E_{Lamb} \approx 500$ eV
$Z\alpha \approx 1$

Quantum **E**lectro- **D**ynamics

Hydrogen
$\langle E \rangle = 1\times10^{10}$ V/cm
$E_k = -13.6$ eV
$\Delta E_{Lamb} \approx 10^{-5}$ eV
$Z\alpha \approx 10^{-2}$

CLTD`s for the Lambshift Experiment on Hydrogen-Like Heavy Ions – Present Status

idea of the experiment: determine absolute transition energy of the Lyman-α line
⇒ most sensitive test of QED (Zα → 1, higher order terms)

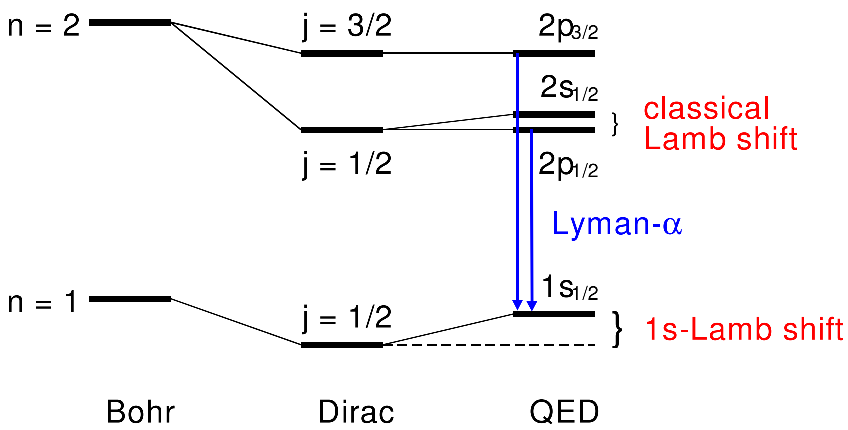

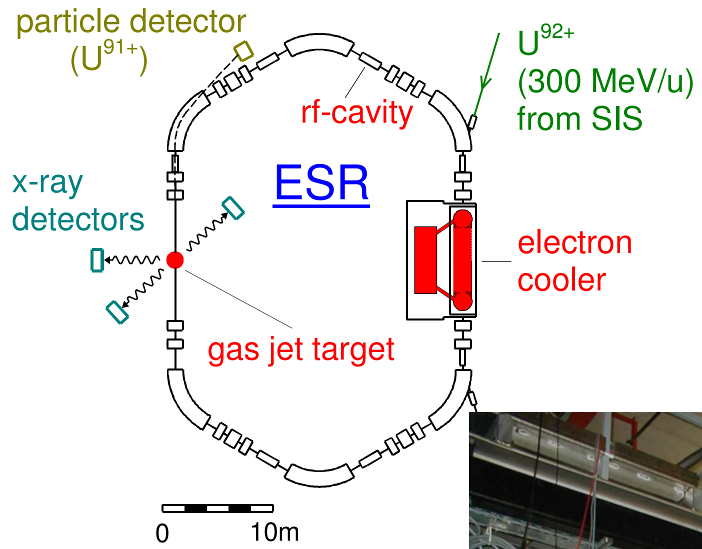

proof of principles for $^{238}U^{91+}$ and $^{207}Pb^{82+}$:

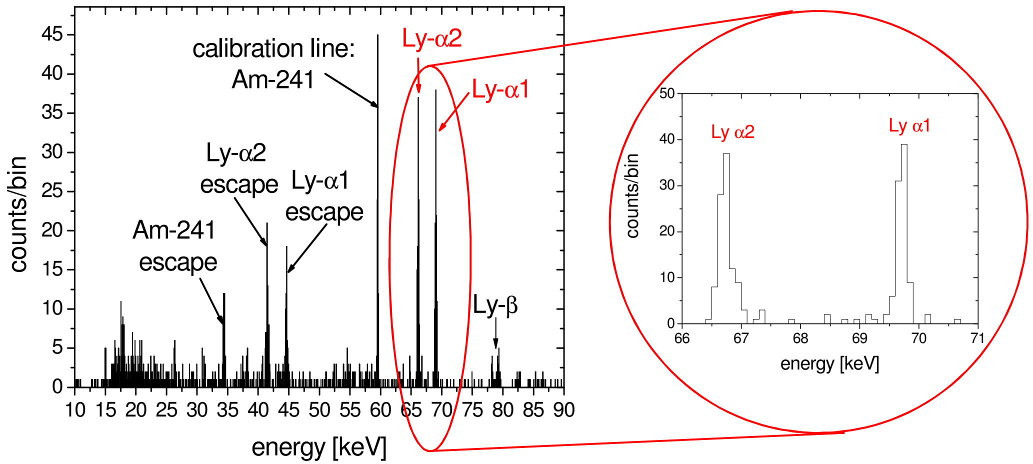

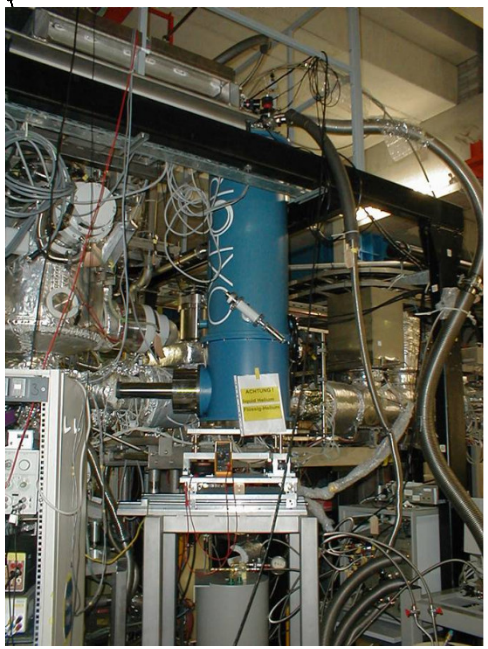

CLTD`s for the Lambshift Experiment on Hydrogen-Like Heavy Ions – Results for Pb^{81+}

results of a joint experiment with the Atomic Physic Group (FOCAL crystal spectrometer):

beam: $^{207}Pb^{82+}$ at 219 MeV/u

overall efficiency: 2.5 x 10^{-7} (only 3 pixels)

V. Andrianov et al.

AIP Conf. Proc. 1185 (2009) 99

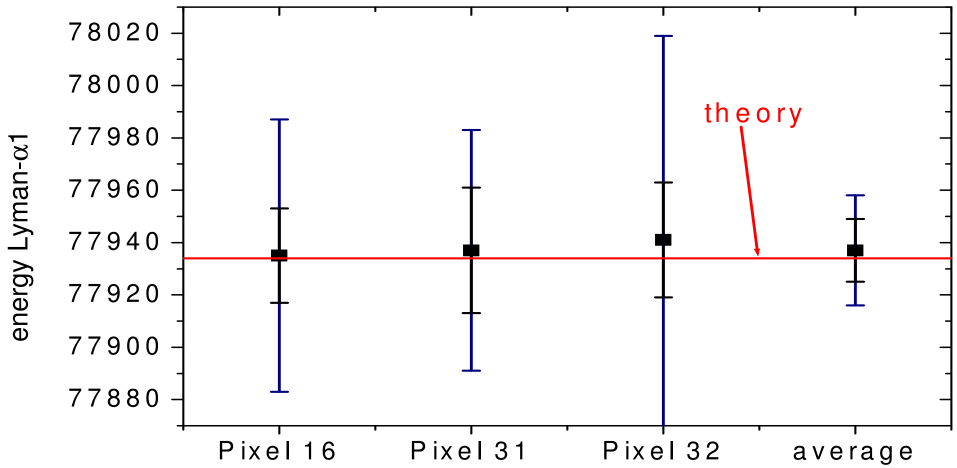

result:

E(Ly-a1) = (77937 $\pm$ 12$_{stat}$ $\pm$ 25$_{syst}$) eV

- good agreement with theory
- systematic uncertainty dominant

CLTD`s for the Lambshift Experiment on Hydrogen-Like Heavy Ions: Results for Au^{78+}

results:

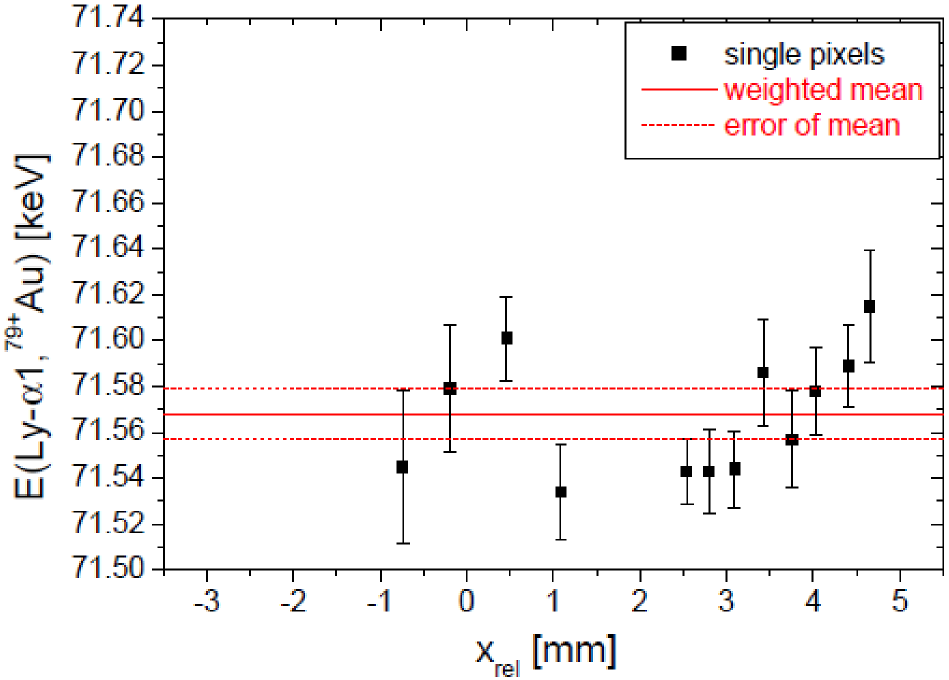

S. Kraft-Bermuth et al.,

J Phys. B50 (2017) 055603

result:

E(Ly-α1) = (71570 ± 4_{stat} ± 11_{syst}) eV

in good agreement with theory:

E(Ly-α1) = (71569 ± 1) eV

⇒ **already sensitive test of QED**

⇒ **systematic error to be improved**

next steps:

- production run with improved statistic and systematic error (aim: 1 eV accuracy)
- at FAIR: HITRAP (highly charged ions at rest)

Perspectives with HITRAP@FAIR

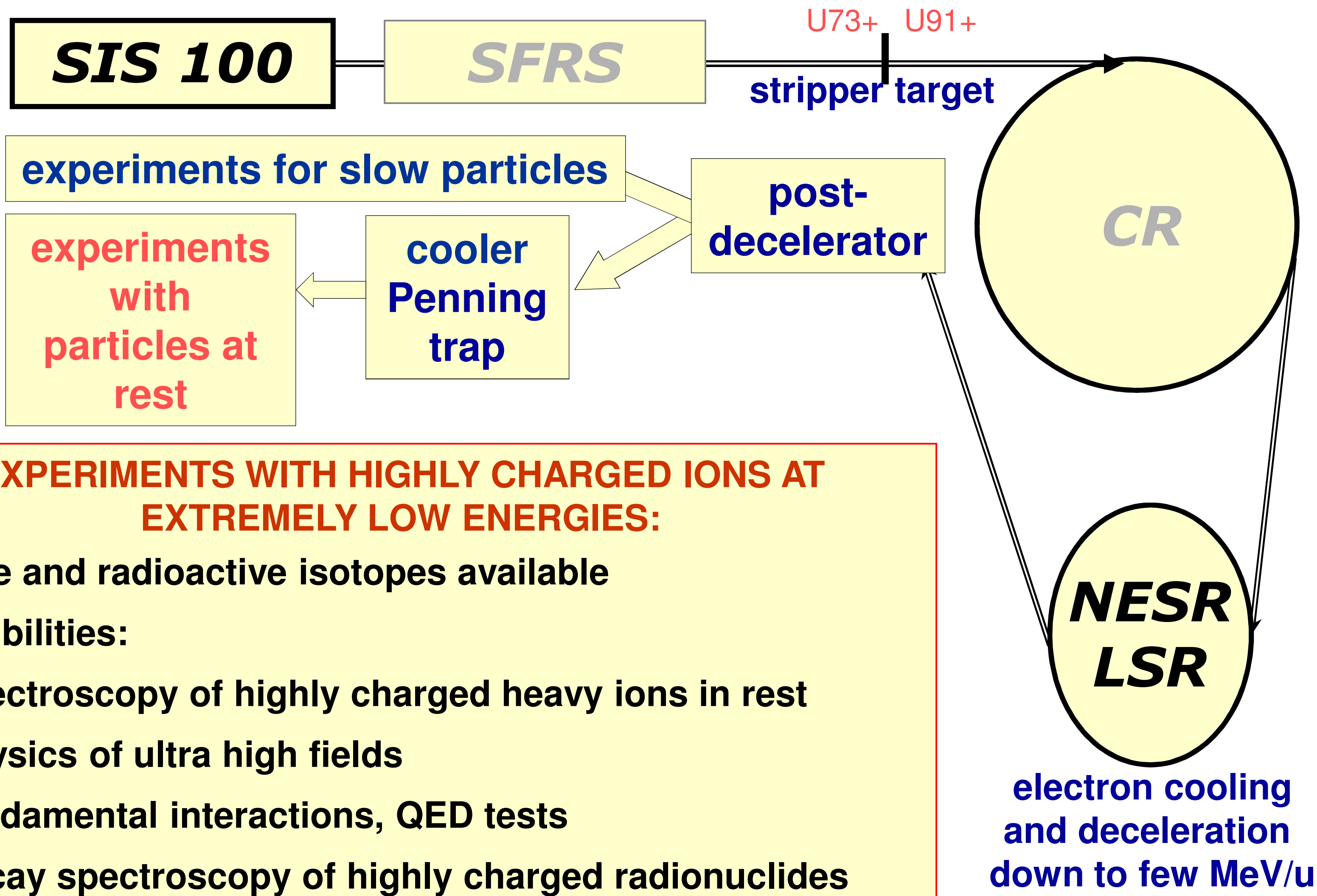

EXPERIMENTS WITH HIGHLY CHARGED IONS AT EXTREMELY LOW ENERGIES:

- stable and radioactive isotopes available
- possibilities:
  - spectroscopy of highly charged heavy ions in rest
  - physics of ultra high fields
  - fundamental interactions, QED tests
  - decay spectroscopy of highly charged radionuclides
  - determine nuclear ground state properties (charge radii)

The 1s-Lamb Shift in Hydrogen-like Ions

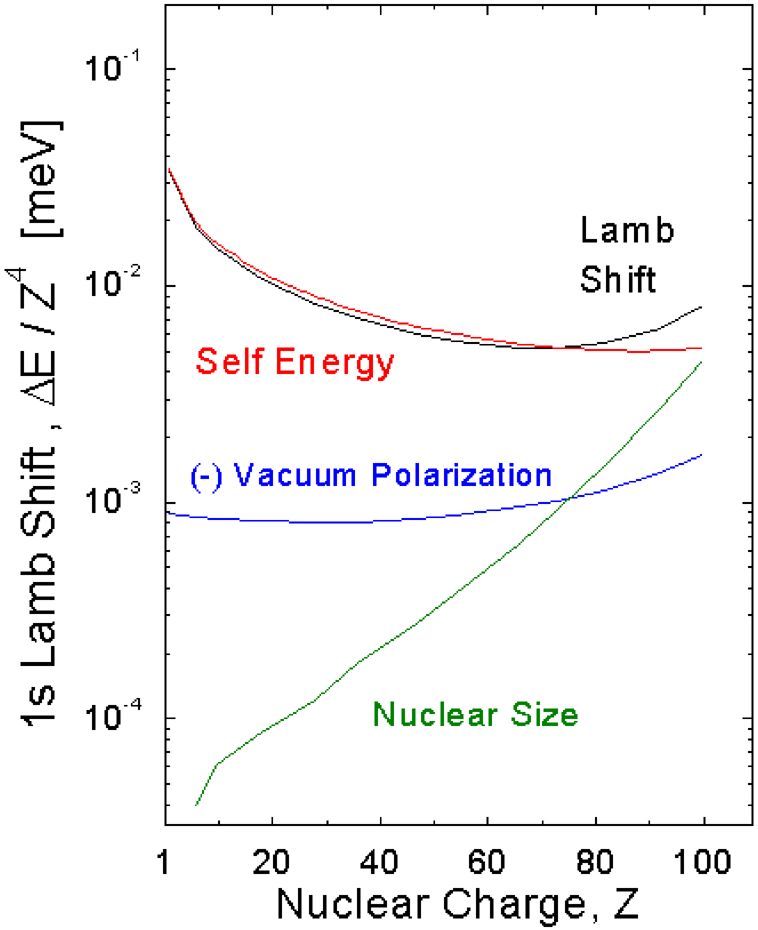

contributions to the 1s Lamb Shift:

for U^{91+}:

Self Energy:	355 eV	(≈ 80%)
Vacuum Polarization:	-89 eV	(≈ -20%)
Nuclear Size	199 eV	(≈ 40%)

determination of nuclear charge radii:

- test QED for stable isotope with known rms-radius
- from Lamb shift measurement for chains of isotopes
  ⇒ determine charge radii with ≤ 1% accuracy

VI. Conclusions

- CLTD`s have substantial advantage over conventional detection systems concerning resolution, linearity, etc.
- CLTD`s for Heavy Ion Physics have been designed and used successfully for experiments
- the results on Z-yield distributions of fission fragments provide important information for nuclear structure-, reactor- and neutrino physics
- CLTD`s were also applied successfully in AMS, stopping power measurements, in-flight mass determination and Lambshift measurements, and have the potential for many further applications,
  as for example for SHE research